APR 29
1957

Registered No. M. 3121

PROCEEDINGS

OF THE

INDIAN ACADEMY OF SCIENCES

VOL. XLV] *SECTION A* [No. 2

FEBRUARY 1957

UNIVERSITY
OF MICHIGAN
APR 24 1957
PHYSICS
LIBRARY

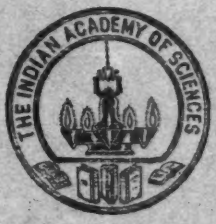

Price Rs. 2 or 3 Sh. *Annual Subscription Rs. 18*

PRINTED AT THE BANGALORE PRESS, BANGALORE CITY, BY C. VASUDEVA RAO
SUPERINTENDENT AND PUBLISHED BY THE INDIAN ACADEMY OF
SCIENCES, BANGALORE

IMPORTANT

In the Year Book of the Academy, on Page 1, under "Secretaries", *substitute* "Prof. K. S. Viswanathan" *in place of* "Prof. G. N. Ramachandran".

THE SPECIFIC HEATS OF SOME METALLIC ELEMENTS

Part III. The Characteristic Frequencies

By Sir C. V. Raman

(*Memoir No.* 93 *from the Raman Research Institute, Bangalore* 6)

Received February 9, 1957

1. Introduction

In Part I of the present series of papers, the experimental data for the specific heat at constant volume of the four metals aluminium, copper, silver and lead were analysed and discussed. The method of analysis was a determination, with the aid of a table of Einstein's specific heat function, of the frequency of atomic vibration which, if assumed to be common to all the atomic oscillators, would give for the specific heat of the solid its observed value at any given temperature. The frequency thus determined is termed the effective average frequency of the atomic oscillators and is itself a function of the temperature. When this is represented as a graph, it discloses a progressive diminution of the frequency in the upper part of the temperature range covered by the data. Considered in relation to the atomic vibration frequencies themselves, this diminution is least conspicuous in the case of *copper*, while the three other metals aluminium, silver and lead form a sequence in which it exhibits an increasing magnitude.

The explanation of these results is not far to seek. The Einstein formula for the energy of an atomic oscillator as a function of its frequency and the expression for the specific heat deduced therefrom by differentiation rest on the assumption that the oscillators are *harmonic*. This assumption is however not strictly justifiable. The expansion of volume which all the metals exhibit with rise of temperature can only be understood if we recognize that the atomic oscillators which are the carriers of the thermal energy are anharmonic in their modes of vibration. Such anharmonicity implies that the vibration frequencies of a quantised oscillator do not form a harmonic sequence but that the successive increments of frequency fall off in a regular progression. Simultaneously also, the dimensions of the oscillator would exhibit a progressive increase which is connected with the magnitude of the vibration and its anharmonicity and hence also with the changes of frequency in a quantitative fashion. It is worthy of remark in this connection that the volume expansion between 0° and 300° absolute

in the case of the four metals under consideration is least for *copper*, being 1%, while the three other metals, aluminium, silver and lead form a sequence in which it progressively increases, being 1·2%, 1·3% and 2·2% respectively for these metals. Thus, there is a clear correlation between the rate of thermal expansion and the rate of change of the atomic vibration frequencies which these metals exhibit at higher temperatures as deduced from their specific heat data.

As is well known, the thermal expansion coefficient of a metal tends to zero at the lowest temperatures and at higher temperatures increases *pari passu* with the specific heat. It follows from these facts and the remarks made above that the specific heats of these metals can be adequately represented by a summation of the Einstein functions for frequencies assumed to be independent of the temperature only over the limited part of the temperature range where the overall expansion of the solid is small and may be ignored without sensible error.

In Part II of the present series of papers, the characteristic frequencies for the four metals were evaluated *by an approximate method* based on their relationship to their elastic constants. As was remarked in that paper, the specific heats thus calculated showed distinct deviations from the observed values in the steeply falling part of the curve where its course is specially sensitive to the values chosen for the frequencies. The need for a more precise evaluation was thereby rendered evident. In the present paper, it will be shown that this revision may be effected by making use of the specific heat data themselves in the lower part of the temperature range.

2. THE CHARACTERISTIC FREQUENCIES

Table I below gives the four characteristic frequencies for the four metals calculated approximately from their elastic constants and used in Part II. In the adjacent columns are shown the revised values adopted in the present paper. The latter have been determined by trial so as to give the best possible fit with the actual course of the specific heat curve in the lower part of the temperature range in each case. Multiplying each frequency by its degeneracy and dividing the sum total by 21, we obtain the average frequency of the atomic oscillators and this is also shown at the foot of each column.

On an examination of the figures in Table I, it will be seen that in all the four cases, the frequencies as now revised exhibit certain general features in common. Their magnitudes follow each other in the order I, III, II and IV. This is also the order to be expected theoretically, for the

TABLE I

Characteristic frequencies in cm.$^{-1}$

Mode	De-generacy	Aluminium		Copper		Silver		Lead	
		From elastic constants	From specific heats	From elastic constants	From specific heats	From elastic constants	From specific heats	From elastic constants	From specific heats
I	3	353	340	260	250	179	179	88	80
II	6	177	200	177	185	109	125	48	45
III	4	287	290	269	215	179	155	87	80
IV	8	145	160	113	120	70	80	30	34
Average ..		211	222	182	175	117	121	54	53

cubic spacings are smaller than the octahedral ones and hence should correspond to higher frequencies of vibration, while the longitudinal oscillations in each case should have a notably higher frequency than the transverse ones. Comparing the frequencies determined from the specific heat data with the approximate values estimated from the elastic constants, we also notice certain general features: the frequency of mode I as now deduced is slightly smaller in all the cases; the frequency of mode II is slightly larger in all the cases except lead; the frequency of mode IV is distinctly larger in all the four cases, while the frequency of mode III is notably diminished in all the cases except aluminium. These alterations have resulted in an increase by a few per cent. of the average of the frequencies for aluminium and silver and a diminution by a few per cent. of the average in the cases of copper and lead. They have also resulted in bringing the four frequencies for each metal into the proper relationships with each other to be expected in physical grounds, already remarked.

3. The Evaluation of the Specific Heats

Using the values of the characteristic frequencies now adopted, the specific heat for each of the four metals has been calculated by summing up the Einstein functions for the four frequencies and adding the contribution from the continuous spectrum, the upper limit of frequency for the latter being the same as the lowest of the four characteristic frequencies. From the specific heats thus evaluated, the effective average frequencies of the atomic oscillators has also been evaluated as a function of temperature.

In Figs. 1, 2, 3 and 4 above, these calculations have been represented graphically. The abscissæ in the graphs are the absolute temperatures, while the ordinates for the specific heats and for the effective average

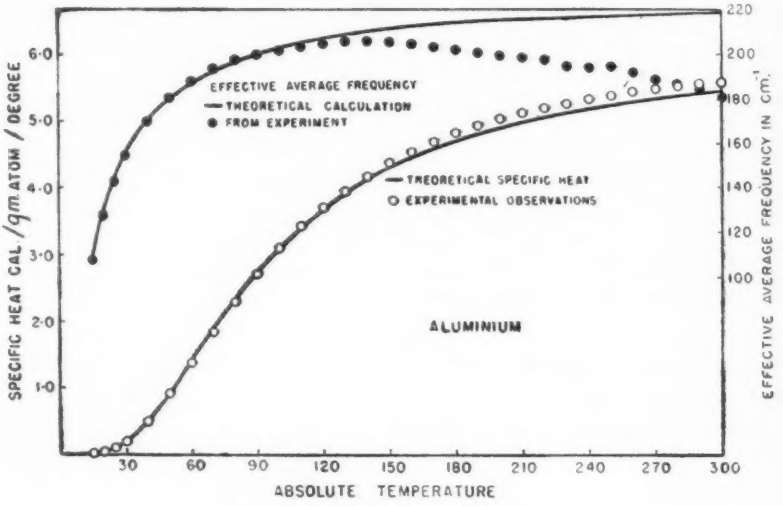

FIG. 1. Specific Heats of Aluminium.

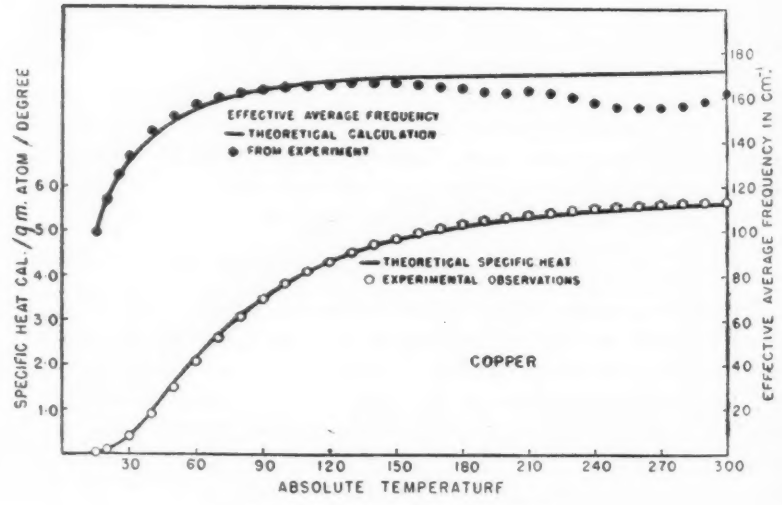

FIG. 2. Specific Heats of Copper.

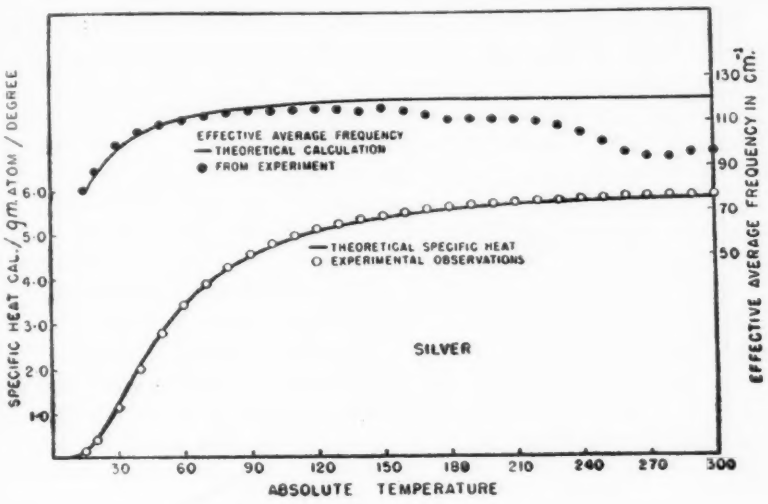

FIG. 3. Specific Heats of Silver.

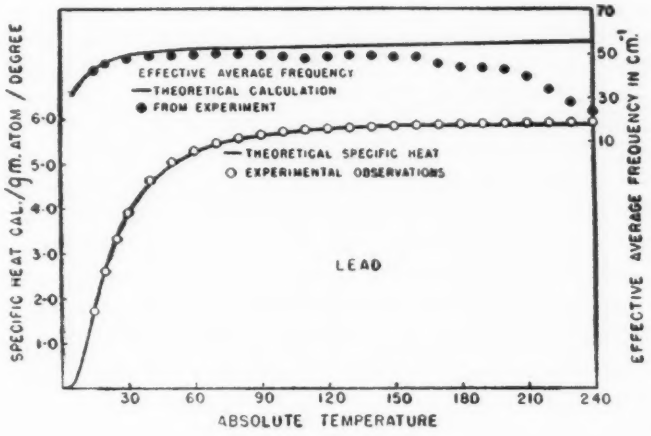

FIG. 4. Specific Heats of Lead.

frequencies appear respectively on the left- and right-hand sides of the figure. It will be seen that the effective average frequency at the upper end of the temperature range is practically the same as the arithmetical average frequency shown at the foot of the columns in Table I in each case.

The experimentally determined values of the specific heat and the effective average frequencies calculated therefrom have also been shown in the graphs alongside of the theoretically computed curves in Figs. 1, 2, 3 and 4. As already stated, the characteristic frequencies employed for the calculation were so chosen as to give the best possible fit with the specific heats in the lower part of the temperature range, *i.e.*, between 15° and 150° absolute in each case. It will be seen that in this part of the temperature range, the observed values fall close to the theoretical curves. On the other hand, in the upper part of the temperature range, *i.e.*, between 150° and 300° absolute, the specific heats observed are consistently higher than the calculated values. The reason for this is evident from the plots of the effective average frequency of atomic vibration. In all the four cases, the atomic vibration frequencies actually effective in the upper part of the temperature range are no longer those deduced from the specific heats at low temperatures but show a progressive diminution with rise of temperature, for the reasons already explained in the Introduction.

SUMMARY

The specific heat data themselves enable us to evaluate more precisely the four characteristic frequencies of each metal determined approximately in Part II from their elastic constants. Making use of the new values, the complete specific heat curve is theoretically deduced and shows good agreement with the observations in the lower part of the temperature range, but deviates observably in its upper part, as is to be expected in view of the progressive fall in the frequency of the atomic oscillators with rise of temperature indicated by the analysis of the data in Part I. This diminution of the frequencies is a consequence of the anharmonicity of the oscillators which also results in the thermal expansion of the metal. Copper, aluminium, silver and lead form a sequence in the order of increasing coefficients of thermal expansion as also in the magnitude of the temperature coefficients of atomic vibration frequency indicated by their specific heat data.

OXIDATIONS WITH SILVER IODIDE DIBENZOATE

Part II. Preparation of *s*-Azo Compounds from Some Aromatic Primary Amines

BY P. S. RAMAN

(*Department of Organic Chemistry, University of Madras, Madras-25*)

Received December 18, 1956

(Communicated by Dr. K. N. Menon, F.A.SC.)

IN a recent paper[1] from this laboratory the use of the Sinomini complex formed from iodine and silver benzoate for the scission of α-glycols was reported. The present communication deals with the oxidation of some substituted anilines. Aromatic primary amines are rapidly oxidised by the reagent with the production of deeply coloured products. A detailed investigation of the action of this reagent on *p*-toluidine, *p*-chloraniline, *p*-bromaniline, *p*-nitroaniline and 2-chloro-4-nitro-aniline has shown that the main product of the oxidation in each case is the corresponding symmetrical azo compound, when molar proportions of silver iodide dibenzoate and the aromatic primary amine are employed. The reaction thus proceeds according to the general equation

$$2R\text{–}NH_2 + 2\,(C_6H_5\text{–}COO)_2\,AgI \longrightarrow R\text{–}N = N\text{–}R + 2\,AgI + 4\,C_6H_5\text{–}COOH.$$

Silver iodo dibenzoate thus constitutes another useful member of a group of oxidising agents like permanganate,[2] ferricyanide,[3] chromic acid anhydride,[4] sodium hypobromite,[5] phenyl iodosoacetate[6] and lead tetraacetate[7, 8] for the oxidation of aromatic primary amines to the corresponding *s*-azo compounds.

The reaction probably involves a free radical mechanism and proceeds through the highly reactive intermediate radical R–NH$^{\bullet}$ which undergoes dimerisation to the hydrazo compound followed by further oxidation to the azo compound.

$$2\,R\text{–}NH_2 \xrightarrow{(C_6H_5\text{–}COO)_2\,AgI} 2\,R\text{–}NH^{\bullet} \longrightarrow R\text{–}NH\text{–}NH\text{–}R \longrightarrow R\text{–}N = N\text{–}R.$$

The intermediate R–NH$^{\bullet}$ may enter into side reactions and this probably accounts for the formation of dark coloured products encountered in the oxidations. This mechanism finds support in the work of Pausacker

and others on the oxidation of aromatic primary amines to azo compounds with phenyl iodosoacetate[6] and lead tetra-acetate[7] for which analogous reaction mechanisms have been proposed by them. The mechanism is also partially supported by the fact that hydrazo benzene is very rapidly oxidised to azo benzene in very high yields (94%) by the action of silver iodide dibenzoate. But aniline itself, on treatment with the complex under mild conditions, gave a dark, gummy product from which only traces of azo benzene could be isolated.

Although the conditions for the maximum yield of the azo compounds were not investigated, the yields obtained in the different cases were fairly good, excepting in the case of *p*-toluidine. The oxidation of *p*-toluidine was very rapid whereas it was relatively slower in the case of *p*-nitroaniline and still slower in the case of 2-chloro-4-nitroaniline. The yields of azo compounds were somewhaht widely different in the case of the different amines; those amines containing electron-attracting groups tend to give relatively higher yields of azo compounds. Thus *p*-toluidine gave 28%, *p*-nitroaniline 44% and 2-chloro-4-nitroaniline 56% of the corresponding azo compound. Benzoic acid, arising from the oxidising agent, was obtained in high yields in all cases after the oxidation.

EXPERIMENTAL

Silver iodide dibenzoate was prepared by warming 9·2 g. (0·04 mole) of silver benzoate and 5 g. (0·04 atom) of iodine in 140 c.c. of dry benzene, with exclusion of moisture. This was cooled to room temperature and the amine (0·02 mole) added either as such or in benzene solution. The mixture in almost all the cases became warm and was afterwards shaken at room temperature and then heated on the water-bath for a short time. By this time the bulky silver iodide dibenzoate got replaced by the heavier silver iodide and the benzene solution became deeply coloured. The hot benzene solution was filtered, the residual silver iodide washed with warm benzene and the combined benzene filtrate worked up for the isolation of the azo derivatives as indicated under the different compounds. The identity of the difierent azo compounds was established by mixed m.p. determinations with authentic specimens prepared according to the general method of Bogoslovskii.[9]

4, 4′-*Dimethyl azo benzene*.—After adding the *p*-toluidine dissolved in dry benzene to the complex, the mixture was shaken for 10 mins. and then heated on the water-bath for about 15 mins. The colour of the benzene solution which was brownish yellow at first turned dark brown by this time. The benzene solution from the reaction was concentrated to small bulk

under reduced pressure, cooled and the crop consisting mostly of benzoic acid was filtered off. The benzene filtrate was brought to dryness and the residue triturated with alcohol. The portion insoluble in alcohol was brown in colour and melted at 135–40°. Wt. 0·6 g. (28%). Crystallisation from alcohol gave pure 4, 4′-dimethyl azo benzene, yellow crystals, m.p. and mixed m.p. 143–44°.

4, 4′-*Dichloro azo benzene*.—*p*-Choraniline in benzene solution was added to the silver iodide dibenzoate complex, mixture shaken for 15 mins. and then heated on the water-bath for 10 mins. Concentration of the dark brown benzene filtrate under reduced pressure to about 40 c.c. and cooling in ice gave the azo compound mixed with benzoic acid. The azo compound (yield 1 g.; 40%; m.p. 180–85°) separated by bicarbonate, crystallised from alcohol and then acetone (charcoal) gave yellow needles, m.p. and mixed m.p. 184–85°.

4, 4′-*Dibromo azo benzene*.—The oxidation of *p*-bromaniline was done exactly as in the case of *p*-chloraniline. The colour of the benzene solution which was brown initially changed to almost dark towards the end. The benzene filtrate, worked up as above, gave 1·4 g. (41%) of the azo compound as a yellowish brown solid, m.p. 197–200°. Crystallisation from acetone (charcoal) gave yellow needles, m.p. and mixed m.p. 203–05°.

4, 4′-*Dinitro azo benzene*.—Powdered *p*-nitroaniline was added to the complex and the mixture heated on the water-bath for 75 mins. The deep red benzene filtrate on concentration to small bulk, gave the azo compound mixed with benzoic acid. Separation by bicarbonate gave the azo compound (1·2 g.; 44%) which on crystallisation from acetone (charcoal) gave orange-red needles, m.p. 223–24°.

2, 2′-*Dichloro*-4, 4′-*dinitro azo benzene*.—After addition of 2-chloro-4-nitroaniline to the complex, the mixture was very gently boiled on the water-bath for 1½ hrs. The benzene solution was brought to dryness under reduced pressure, residue treated with bicarbonate solution and then triturated with cold alcohol. Filtration gave a brown product (1·9 g.; 56%) melting at about 270°. Crystallisation from benzene gave the azo compound as fine, brownish red crystals, m.p. and mixed m.p. 275–76°.

Azo benzene from hydrazo benzene.—Hydrazo benzene (3·7 g.) was added to the complex prepared as above and after shaking the warm mixture for 15 mins., it was heated on the water-bath for 10 mins. The colour of the benzene layer which immediately changed to yellow, turned reddish yellow and finally reddish brown. The filtered benzene solution was brought to

dryness, the residue taken up in ether, washed with bicarbonate solution and then water, the ether solution dried with anhydrous sodium sulphate and the solvent removed. The residue on a single crystallisation from dil. alcohol gave 3·45 g. of azo benzene as orange-red crystals, m.p. and mixed m.p. 67–68°.

ACKNOWLEDGMENT

My thanks are due to Prof. K. N. Menon for his valuable help and suggestions in this work.

SUMMARY

The formation of *s*-azo compounds by the oxidation of some aromatic primary amines by silver iodide dibenzoate is described. The reaction probably proceeds through a free radical mechanism in which the highly reactive R–NH• radical plays a part.

REFERENCES

1. Raman, P. S. .. *Proc. Ind. Acad. Sci.*, 1956, **44**, 321.
2. Glaser, C. .. *Z. chem.*, 1866, **9**, 308; *Ann.*, 1867, **142**, 364.
3. Bamberger, E. and Meimberg, F. *Ber. deut. chem. Ges.*, 1893, **26**, 497.
4. Bornstein, E. .. *Ibid.*, 1901, **34**, 1271;
   Meyer, F. and Dahlem, K. .. *Ann.*, 1903, **326**, 338.
5. Meigen, W. and Nottebohm, E. *Ber. deut. chem. Ges.*, 1906, **39**, 744.
6. Pausacker, K. H. .. *J. Chem. Soc.*, 1953, 1989;
   Barlin, G. B., Pausacker, K. H. and Riggs, N. V. .. *Ibid.*, 1954, 3122.
7. ——— and Scroggie, J. G. *Ibid.*, 1954, 4003.
8. Baer, E. and Tosoni, A. L. .. *J. Am. Chem. Soc.*, 1956, **78**, 2857.
9. Bogoslovskii, B. M. .. *J. Gen. Chem.*, 1946, **16**, 193.

NUMERICAL CALCULATIONS ON THE NEW APPROACH TO THE CASCADE THEORY—I

By S. K. Srinivasan and N. R. Ranganathan

(Department of Physics, University of Madras)

Received December 3, 1956

(Communicated by Dr. Alladi Ramakrishnan, F.A.SC.)

Abstract

In the new approach to the cascade theory suggested by Alladi Ramakrishnan and one of us (S. K. S.), we deal with the number of electrons produced between 0 and t in a soft cascade, each of these electrons having an energy greater than E at the point of its production as contrasted with the usual approach where we are interested in the number of electrons with energy greater than E at t. We present here numerical calculations of the mean numbers on the basis of the new approach.

In a previous paper (1956) in these proceedings (hereafter referred to as Paper I), Ramakrishnan and one of us (S. K. S.) suggested a new approach to cascade theory which yields equations having elegant asymptotic solutions. In the normal approach we are interested in $n(E; t)$ the number of particles above a certain energy E at a particular thickness t in a shower initiated by a particle of known energy or energy distribution. On the other hand, we now ask for $N(E; t)$ the number of particles produced between 0 and t each with energy greater than E at the point of its production. It is well known that $n(E; t)$ and $N(E; t)$ are stochastic variates and a comprehensive treatment should deal with their probability distribution functions. A more limited and tractable problem is to obtain the first and second moments of the distribution. In the case of electron-photon showers the first and second moments of $n(E; t)$ have been tabulated by other workers.* We now here present the numerical calculations relating to the first moment of $N(E; t)$.

In Paper I, Ramakrishnan and one of us (S. K. S.) have proved that the mean number of electrons produced between 0 and t with their primitive energies above E, in a shower initiated by a single electron of energy E_0 is given by

---

* For a comprehensive account of the treatment, see Ramakrishnan and Mathews (1954).

$$\epsilon\{N(E|E_0;\ t)\}$$

$$= \frac{1}{2\pi i}\int_{\sigma-i\infty}^{\sigma+i\infty} \frac{B_s C_s}{\mu_s - \lambda_s}\left(\frac{E_0}{E}\right)^{s-1} \cdot \frac{1}{s-1}\left\{\frac{1-e^{-\lambda_s t}}{\lambda_s} - \frac{1-e^{-\mu_s t}}{\mu_s}\right\} ds \quad (1)$$

where

$$B_s = 2\left\{\frac{1}{s} - \left(\frac{4}{3}+\alpha\right)\frac{1}{(s+1)\ (s+2)}\right\}. \quad (2)$$

$$C_s = \frac{1}{s+1} + \left(\frac{4}{3}+\alpha\right)\frac{1}{s\,(s-1)}. \quad (3)$$

$$\lambda_s = \tfrac{1}{2}(A_s + D) - \tfrac{1}{2}\{(A_s - D)^2 + 4\ B_s C_s\}^{\frac{1}{2}}. \quad (4)$$

$$\mu_s = \tfrac{1}{2}(A_s + D) + \tfrac{1}{2}\{(A_s - D)^2 + 4\ B_s C_s\}^{\frac{1}{2}}. \quad (5)$$

$$A_s = \left(\frac{4}{3}+\alpha\right)\left\{\frac{d}{ds}\log|\bar{s}+\gamma-1+\frac{1}{s}\right\} + \tfrac{1}{2} - \frac{1}{s\,(s+1)}. \quad (6)$$

$$D = \frac{7}{9} - \frac{1}{6}\alpha,\ \alpha = \cdot 0246. \quad (7)$$

For fairly large thicknesses (say $t \geqslant 4$), we can neglect the term containing $e^{-\mu_s t}$ and (1) can be written as

$$\epsilon\{N(E|E_0;\ t)\} = \frac{1}{2\pi i}\int_{\sigma-i\infty}^{\sigma+i\infty} \frac{B_s C_s}{\mu_s \lambda_s} \cdot \frac{1}{s-1} \cdot \left(\frac{E_0}{E}\right)^{s-1} ds$$

$$- \frac{1}{2\pi i}\int_{\sigma-i\infty}^{\sigma+i\infty} \frac{B_s\ C_s}{\mu_s - \lambda_s} \cdot \frac{e^{-\lambda_s t}}{\lambda_s\,(s-1)}\left(\frac{E_0}{E}\right)^{s-1} ds$$

$$= \frac{1}{2\pi i}\int_{\sigma-i\infty}^{\sigma+i\infty} e^{\phi_1(s)}\, ds - \frac{1}{2\pi i}\int_{\sigma-i\infty}^{\sigma+i\infty} e^{\phi_2(s;\,t)}\, ds \quad (8)$$

where

$$\phi_1(S) = \log\frac{B_s C_s}{\mu_s \lambda_s} - \log(s-1) + y(s-1);\ y = \log\frac{E_0}{E} \quad (9)$$

$$\phi_2(S;\ t) = \log\frac{B_s C_s}{(\mu_s - \lambda_s)\lambda_s} - \log(s-1) + y(s-1) - t\lambda_s \quad (10)$$

Noting that $\epsilon\{N(E/E_0; t)\}$ is a function only of E_0/E or $y = \log E_0/E$ we can write it as $\epsilon\{N(y; t)\}$. We next observe that as $t \to \infty$ the second intergral tends to 0 and hence we have

$$\epsilon\{N(y; \infty)\} = \frac{1}{2\pi i}\int_{\sigma-i\infty}^{\sigma+i\infty} e^{\phi_1(s)}\, ds \tag{11}$$

As $s \to 2$, $\lambda_s \to 0$ and $B_s C_s/\mu_s$ remains finite and non zero at $s = 2$. Hence $\phi_1(s)$ and $\phi_2(s; t) \to +\infty$ as $s \to 2$. From (2) to (7), it follows that for very large real part of s,

$$A_s \simeq \left(\frac{4}{3} + a\right)\left(\log s + \gamma - 1 + \frac{1}{2s}\right) + \tfrac{1}{2}$$

$$B_s \simeq \frac{2}{s}$$

$$C_s \simeq \frac{1}{s+1}$$

$$\lambda_s \simeq D - \frac{B_s C_s}{A_s - D} \simeq D - \frac{2}{\left(\frac{4}{3} + a\right) s(s+1)\log s}$$

$$\mu_s \simeq A_s + \frac{B_s C_s}{A_s - D} \simeq A_s + \frac{2}{\left(\frac{4}{3} + a\right) s(s+1)\log s} \tag{12}$$

This

$$\log \frac{B_s C_s}{\mu_s \lambda_s} - \log(s-1)$$

and

$$\log \frac{B_s C_s}{(\mu_s - \lambda_s)\lambda_s} - \log(s-1) - t\lambda_s$$

tend to $-\infty$ logarithmically. Since $y(s-1) \to +\infty$ much more rapidly, $\phi_1(s)$ and $\phi_2(s; t)$ tend to $+\infty$, as $s \to \infty$. Hence ϕ_1 and ϕ_2 must have a minimum as s increases along the real axis from 2 to ∞. Let s_1 and s_2 be the points at which

$$\left(\frac{d\phi_1}{ds}\right)_{s=s_1} = 0, \left(\frac{\partial\phi_2}{\partial s}\right)_{s=s_2} = 0 \tag{13}$$

We can shift the line of integration in each of the integrals so that it passes through the saddle points. This can always be achieved since the only restriction on the line of integration is that it should be to the right of imaginary axis and also to the right of all singularities, *i.e.*, $\sigma > 2$. Having chosen the contour to pass through the saddle point, we have the well-known approximation of the saddle point method obtained by replacing each of the functions ϕ_1 and ϕ_2 by the first three terms of its Taylor expansion about the saddle point.

Thus

$$\phi_1(s) \simeq \phi_1(s_1) - \xi^2 \left(\frac{d^2\phi_1}{ds^2}\right)_{s=s_1} \tag{14}$$

$$\phi_2(s;t) \simeq \phi_2(s_1;t) - \eta^2 \left(\frac{\partial^2\phi_2}{\partial s^2}\right)_{s=s_2} \tag{15}$$

where

$$i\xi = s - s_1 \text{ in (14) and } i\eta = s - s_2 \text{ in (15).}$$

Substituting (14) and (15) in (8), we have

$$\epsilon\{N(y;t)\} = \frac{1}{2\pi}\int_{-\infty}^{+\infty} e^{\phi_1(s_1) - \frac{1}{2}\xi^2\phi_1''(s_1)}\, d\xi$$

$$- \frac{1}{2\pi}\int_{-\infty}^{+\infty} e^{\phi_2(s_2;t) - \frac{1}{2}\eta^2\phi_2''(s_2;t)}\, d\eta \tag{16}$$

(primes indicate differentiation with respect to s).
Hence

$$\epsilon\{N(y;t)\} = \frac{e^{\phi_1(s_1)}}{\sqrt{2\pi\phi_1''(s_1)}} - \frac{e^{\phi_2(s_2;t)}}{\sqrt{2\pi\phi_2''(s_2;t)}} \tag{17}$$

The mean numbers $\epsilon\{N(y;t)\}$ for various values of y and t have been calculated numerically using (17). In order to obtain the saddle points, it was found necessary to sub-tabulate at intervals of ·025, the basic functions A_s, B_s, C_s, λ_s and μ_s tabulated by Janossy and Messel (1951) at intervals of ·1. The mean number of electrons produced in infinite thickness and fairly large thickness are given in the following table. For convenience of comparison, we have also tabulated $\epsilon\{n(y;t)\}$, the mean number of electrons that exist at t with an energy above E.†

† These are taken from the table of Ramakrishnan and Mathews (1954).

$\epsilon\{N(y;t)\}$

$\epsilon\{n(y;t)\}$ is given in brackets.

y/t	4	6	8	16	∞
8	293 (94·2)	528 (149)	851 (146)	1372	1406
7	124 (48·8)	249 (61·3)	355 (49·6)	502	508
6	64·5 (23·4)	111 (22·9)	146 (15·1)	183	184·5
5	30·6 (10·2)	41·6 (7·55)	57·9 (4·01)	66·4	66·5
4	10·9 (3·85)	14·7 (2·11)	18·9 (1·897)	20·51	20·53
3	6·65 (1·21)	7·86 ·475)	8·56 (·160)	8·82	8·82

$\epsilon\{N(y;t)\}$ unlike $\epsilon\{n(y;t)\}$ has an interesting asymptotic property. While $\epsilon\{n(y;t)\} \to 0$ as $t \to \infty$, $\epsilon\{N(y;t)\}$ tends to a finite value for any finite y as $t \to \infty$. The smaller the y we observe from the table, the more quickly does $\epsilon\{N(y;t)\}$ approach the limit. For almost all the y given in the table the limit is nearly reached at $t = 16$.

For small thickness, we cannot neglect the term containing $e^{-\mu t}$ in (1). Then the saddle point formula as adapted here cannot be applied to this term. An alternative method of calculation of (1) for small thickness is being attempted and the mean numbers for small thickness will be reported in a subsequent contribution.

We are deeply indebted to Dr. Alladi Ramakrishnan for suggesting this problem.

References

Janossy and Messel, H. .. *Proc. Roy. Irish Acad.*, 1951, **54**, 217.

Ramakrishnan, Alladi and Mathews, P. M. *Prog. Theo. Physics*, 1954, **11**, 95.

——— and Srinivasan, S. K. .. *Proc. Ind. Acad. Sci. A*, 1956, **44**, 263.

ON THE DETERMINATION OF THE SLOWING DOWN LENGTH IN ORDINARY WATER USING A PULSED NEUTRON SOURCE

By R. Ramanna and M. P. Navalkar
(*Atomic Energy Establishment, Bombay*)

Received November 22, 1956
(Communicated by Prof. B. Peters, F.A.SC.)

Introduction

A method of determining the slowing down age in ordinary water from a fast neutron source to thermal energy, using a pulsed neutron source is described. The fast neutrons were produced from the D-Be reaction using a cascade generator. This reaction emits neutrons of maximum energy of 4·5 Mev with a peak at about 3·5 Mev. Pulsed neutron methods have been used by earlier workers in the measurement of the mean life of thermal neutrons in water (Haworth *et al.*, 1942),[1] (Von Dardel *et al.*, 1953),[2] (Antonov *et al.*, 1955),[3] the diffusion length of ordinary water and other substances (Von Dardel, 1953),[4] the diffusion parameters of ordinary water (Von Dardel *et al.*, 1954)[5] and the diffusion and the slowing down constants of ordinary water and beryllium oxide (Ramanna *et al.*, 1956).[6]

Theory

The slowing down of neutrons in a moderating medium can be explained either on the Age Theory or Multi-Group Theory. The Age Theory assumes a continuous process of energy loss of source neutrons to thermal energy whereas in the Multi-Group Theory the energy interval from source to thermal is divided into finite number and there is no energy degradation of neutrons in any group until they go over to the next group. The Multi-Group Theory approximates to the Age Theory when the number of energy intervals tend to infinity. But in the case of light moderators like water where the number of collisions to thermalise is small, the Age Theory is a poor approximation to the slowing down process.

The spatial and time distribution of thermal neutrons from a pulsed source of fast neutrons has been given on the two theories as follows (Mani and Iyengar, 1957)[7]

Age Theory

$$\rho_s(r, t) = \frac{S_0}{8\pi^{3/2}} e^{-(t-\tau_{st})/\tau_{ss}}$$

$$\times \frac{\exp.\left[-\dfrac{r^2}{4\{\tau_0 + L_s^2(t-\tau_{cf})/\tau_{cs}\}}\right]}{[\tau_0 + L_s^2(t-\tau_{cf})/\tau_{cs}]^{3/2}} \qquad (1)$$

where

τ_{cf} = Slowing down time of source neutrons to thermal energy.

τ_{cs} = Mean life of thermal neutrons in the moderator.

τ_0 = Age of source neutrons to thermal energy.

L_s = Diffusion length of thermal neutrons in the moderator.

S_0 = Source strength.

Two Group Theory

$$\rho_s(r,t) = \frac{\tau_{cs}S_0}{2\pi^2\beta r}\left[e^{\frac{-t}{\tau_{cs}}} I(a_s, \sqrt{\mu}) - e^{\frac{-t}{\tau_{cf}}} I(a_f, \sqrt{\mu})\right] \qquad (2)$$

where

$$\beta = \tau_{cs} - \tau_{cf} \qquad \mu = \frac{\tau_{cs}L_f^2 - \tau_{cf}L_s^2}{\beta}$$

$$a_s = \frac{L_s^2 t}{\tau_{cs}} \qquad a_f = \frac{L_f^2 t}{\tau_{cf}}$$

$$I(a,\sqrt{\mu}) = \frac{\pi}{4\mu r} e^{\frac{a}{\mu}}\left[e^{\frac{-r}{\sqrt{\mu}}}\left\{1 - erf.\left(\sqrt{\frac{a}{\mu}} - \frac{r}{2\sqrt{a}}\right)\right\} - e^{\frac{r}{\sqrt{\mu}}}\left\{1 - erf.\left(\sqrt{\frac{a}{\mu}} + \frac{r}{2\sqrt{a}}\right)\right\}\right] \qquad (3)$$

and

$$\frac{\sqrt{\pi}}{2} erf(x) = \int_0^x e^{-u^2} du.$$

where the subscript 's' denotes the slow term and 'f' denotes the fast term.

$I(a,\sqrt{\mu}) \approx e^{\frac{a}{\mu}} e^{\frac{-r}{\sqrt{\mu}}}$ upto a time t_1 after which it decreases rapidly. Since $\tau_{cf} \ll \tau_{cs}$ after a time t_2, $I(a_f,\sqrt{\mu}) \ll I(a_s,\sqrt{\mu})$ and can be neglected. Hence between t_1 and t_2, t_2 being less than t_1

$$\rho_s(r,t) = \frac{\tau_{cs}S_0}{4\pi\mu\beta r^2} e^{\frac{-r}{\sqrt{\mu}}} e^{\frac{-t}{\tau_{cs}}}\left[1 - \frac{L_s^2}{\mu}\right] \qquad (4)$$

and so

$$\frac{d}{dt}\log \rho_s(r, t) = -\frac{1}{\tau_{cs}}\left[1 - \frac{\tau_{cf} - \tau_{cs}}{\tau_{cf}L_s^2 - \tau_{cs}L_f^2}\, L_s^2\right] \tag{5}$$

Unlike the Two Group Theory, the Age Theory expression does not show such an exponential character in any interval of time.

Also

$$\frac{d}{dr}\log \frac{r^2\rho_s(r, t)}{S_0} = -\frac{1}{\sqrt{\mu}} \tag{6}$$

But

$$\mu = \frac{\tau_{cs}L_f^2 - \tau_{cf}L_s^2}{\tau_{cs} - \tau_{cf}} \tag{7}$$

$$\approx L_f^2 \text{ (since } \tau_{cf} \ll \tau_{cs})$$

where L_f^2 = Square of the slowing down length of source neutrons to thermal energy.

Therefore, L_f can be determined using the above expression from a measurement of the spatial distribution of neutron from a pulsed source.

Experimental Arrangement

The neutron pulsing system.—The fast neutron bursts were produced by pulsing the extraction electrode of the radio frequency ion source of the cascade generator. The pulse width was kept at 19 μ-sec. and the repetition rate at 560 cycles per second.

Detector.—The thermal neutrons were detected by means of a lithium iodide scintillation counter. The crystal (1·25 cm. in diameter, 1 cm. long) was mounted at the end of a long perspex rod (3 ft. long, 1 in. in diameter) which was attached to the photo cathode of a 6262 E.M.I. photo multiplier. The pulse from the disintegration of lithium due to thermal neutrons is much higher than the background radiation and can thus be easily discriminated. The light guide assembly was provided with a spigot at its end so that the position of the crystal could be fixed at known distances and in the same plane from the centre of the target. This was done by inserting the spigot into various positions on a perspex strip attached to the target holder. The strip was provided with holes at fixed positions to take in this spigot and was so arranged that it was kept at the centre of the assembly. A rectangular tank (60 cms. cube) of perspex was filled with approx. 55 gallons of distilled water. The sides and bottom of the tank were covered with ·5 mm.

thick cadmium on the outside to absorb thermal neutrons entering or leaving the tank. The block diagram of the experimental set-up is given in Fig. 1.

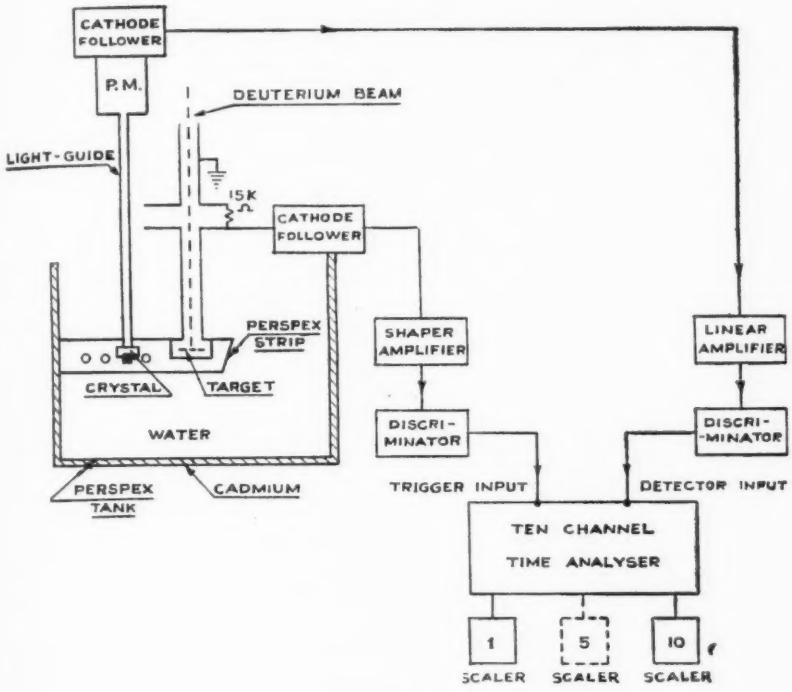

FIG. 1

Block Diagram of the Experimental Apparatus

The Time Analyser.—The thermal neutrons were analysed in time by a 10 channel time analyser (Iyengar, 1956).[8] For the experiment each channel width was adjusted to 54 μ-sec. with an initial delay of 200 μ-sec. In order to get more points in between, the initial decay was shifted to 227 μ-sec. keeping the channel width same. The two sets of readings were normalised by the thermal neutron counts taken in the same interval of time for both the delays. In this case the interval of time was 0–150 μ-sec.

Experimental neutron distribution for some of the detector positions is shown in Fig. 2 *a* and 2 *b* while the theoretical curves on both the Age and the Two Group Theory for $r = 30$ cms. are given in Fig. 2 *c*. It is

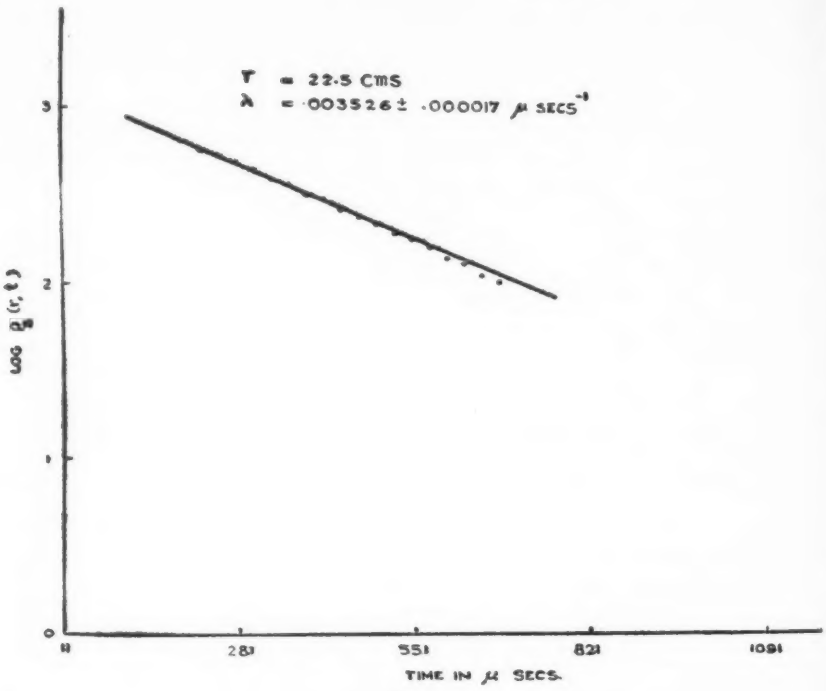

FIG. 2 *a*

noticed that in the region between 200 and 500 μ-sec. the experimental distribution plotted on a log scale is a straight line when the detector is at 22·5 cms. from the source. The straight line portion increases in time duration as the detector is moved away from the source. The values of the decay constants at various detector positions from the source have been determined by least square fitting and are given in Table I.

Calculations of the decay constant were made on both Age and Two Group Theories. The constants used in the calculations were as follows: Using Marshak's formula for the age of source neutrons to indium energy and correcting it for thermal energy, the value obtained for age is about 39 cms.[2] for 3 Mev. and 44 cm.[2] for 3·5 Mev. mono-energetic neutrons. Taking a value of about 41 cms.[2] for age, $\tau_{cs} = 216\,\mu$-seconds,[3] $\tau_{cf} = 10\,\mu$-seconds,[9] $L_s = 2{\cdot}88$ cms.[9] and using expression (5), the Two Group Theory gives a decay constant of $0{\cdot}0037\,\mu$-sec.$^{-1}$ which is in better agreement with the experimental value. Unlike the Two Group Theory, the Age Theory gives different decay constants at different detector positions while those obtained

TABLE I

Distance r from the source in cms.	Time in which λ is calculated in μ-sec.	Decay constant λ μ-sec.$^{-1}$	Error in λ $d\lambda$
20	227–389	0·003558	$\pm$ 0·000015
22·5	227–497	0·003526	$\pm$ 0·000017
25	227–497	0·003450	$\pm$ 0·000019
27·5	227–497	0·003455	$\pm$ 0·000024
30	335–686	0·003434	$\pm$ 0·000022
32·5	335–686	0·003429	$\pm$ 0·000024

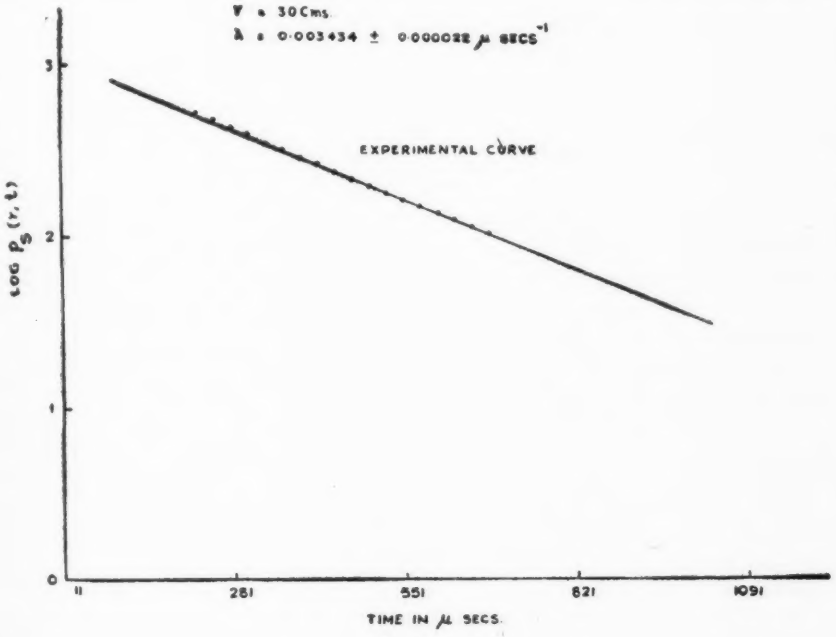

FIG. 2 *b*

experimentally are independent of the detector positions as long as they are greater than 22·5 cms., thus showing that the Two Group Theory

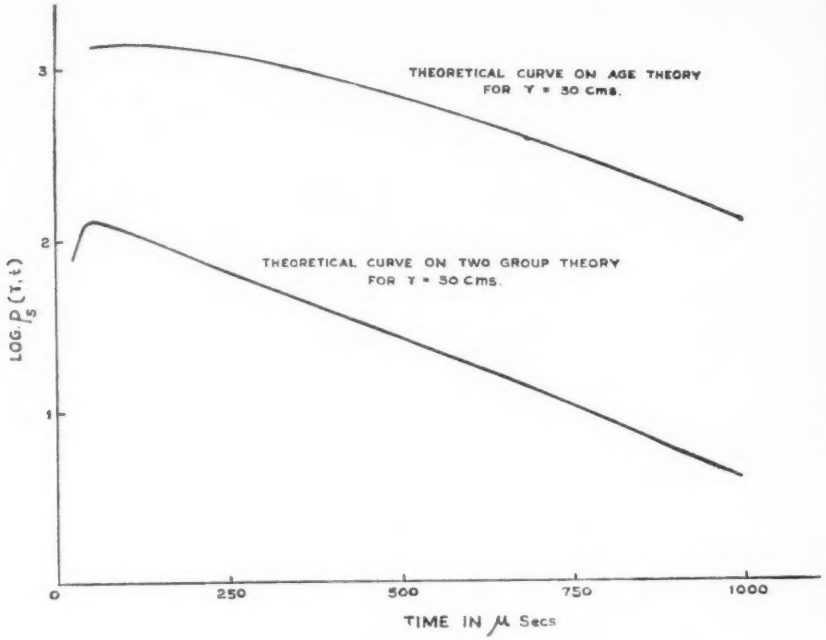

FIG. 2c

applies better than Age Theory in case of water. The disagreement of Age Theory is to be expected since it is well known that the Age Theory is inapplicable in case of light moderators like water. The experimental value of the decay constant is in agreement with the value obtained previously, (Ramanna *et al.*, 1956).[6]

The values of the decay constants at detector distances of 10 and 15 cms. from the source are much higher than expected on the Two Group Theory. This may be explained on the basis that at such close distances there is a large concentration of fast neutrons which decay more rapidly than thermal neutrons and hence give higher value of the decay constant. The decay constant therefore decreases with distance from the source and then remains constant.

Fig. 3 shows $\log \frac{r^2 \rho_s (r, t)}{S_0}$ against 'r' and is seen to be a straight line. The slope of this line at various times is given in Table II. Using the average value of these slopes and taking $\tau_{cs} = 216$ μ-sec,[3] $\tau_{cf} = 10$ micro-sec.[9]

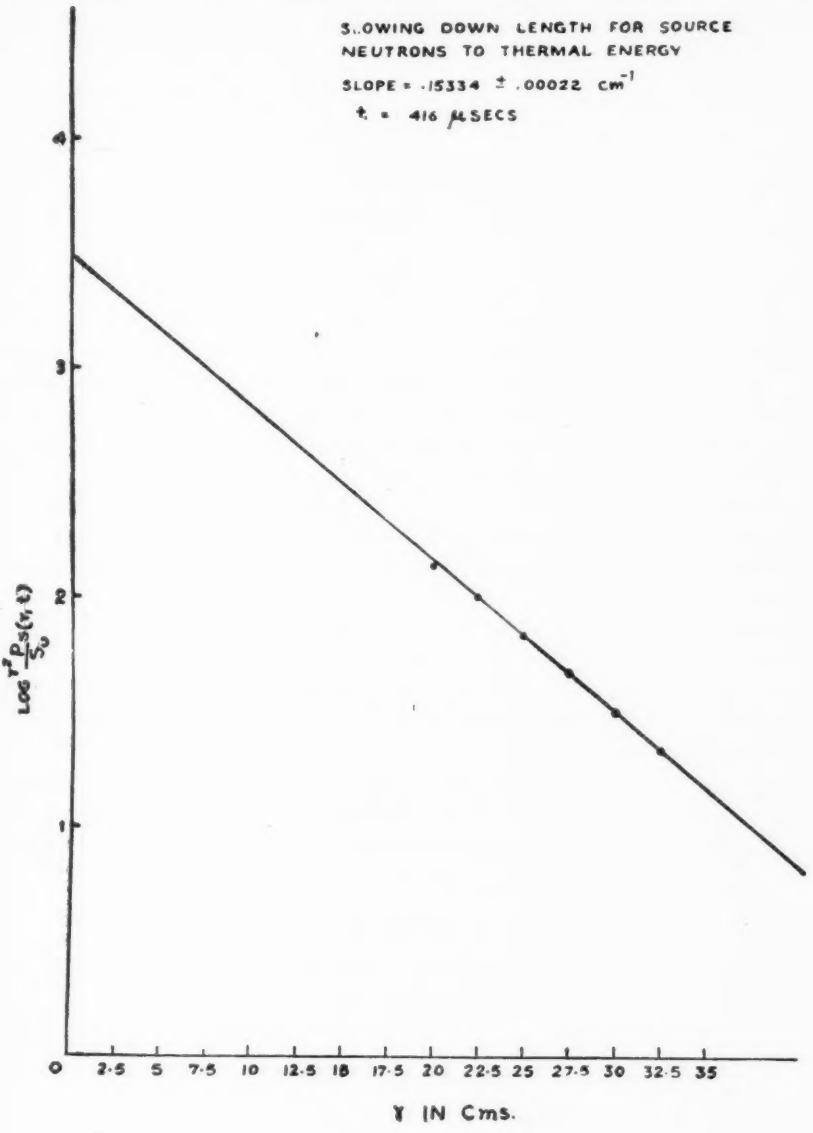
SLOWING DOWN LENGTH FOR SOURCE NEUTRONS TO THERMAL ENERGY
SLOPE = .15334 ± .00022 cm⁻¹
t = 416 μSECS
Log r² Ps(r,t) / S0
4
3
2
1
0
2·5
5
7·5
10
12·5
15
17·5
20
22·5
25
27·5
30
32·5
35
r IN Cms.

FIG. 3

TABLE II

Time in microseconds	Slope of $\log \frac{r^2\rho_s(r,t)}{S_0} - r$	Error in the slope
362	0·15307	± 0·00021
416	0·15334	± 0·00022
470	0·15297	± 0·00022

and $L_s = 2{\cdot}88$ cms.[9] in expression (7), we get the age of source neutrons to the thermal energy as 41·05 cms.[2] The value of the age changes to 39·47 cms.[2] when τ_{cf} is taken as 20 μ-sec. If we use the approximation in expression (7), *i.e.*, $\tau_{cf} = 0$, we obtain 42·65 cms.[2] as the value for the age. It can be noticed that in altering the value of τ_{cf}, the value of the age does not change more than ± 4·0%. The statistical error due to counting is very small compared to the above error and can be neglected. It is unlikely that the value quoted above for age 41·05 cms.[2] has been determined to better than ± 4·0%, taking into account both the approximations involved in theory and the experimental errors introduced due to the finite dimensions of the detector, the source and the moderator assembly. It can, therefore, be concluded that the experimental value obtained for age by this method is consistent with the value expected for the D-Be neutrons.

We wish to express our thanks to Mr. S. B. D. Iyengar, Mr. G. S. Mani and Mr. P. K. Iyengar for helpful discussions. Our thanks are also due to Mr. S. K. Ambardekar for running the accelerator and Mr. F. R. Bhathena for his help in taking readings with the time analyser.

REFERENCES

1. Haworth, L. J., Luebke, E. A. and Manley, J. H. — *Phys. Rev.*, 1942, **61**, 152.
2. Von Dardel and Waltner, A. W. — *Ibid.*, 1953 **91**, 1284.
3. Antonov, A. V., Isakoff, A. I., Murin, I. D., Neupocoyev, B. A., Frank, I. M., Shapiro, F. L. and Shtranich, I. V. — *Geneva paper* 8/P/661.
4. Von Dardel, G. F. .. — *Thesis Goteborg*, 1953.

5. Von Dardel, G. F. and Sjostrand, N. G. — *Phys. Rev.*, 1954, **96**, 1245.

6. Ramanna, R., Mani, G. S., Iyengar, P. K., Iyengar, S. B. D. and Joshi, B. V. — *J. Nuclear Energy*, 1956, **2** (3), 145.

7. Iyengar, S. B. D. and Mani, G. S. — *Proc. Ind. Acad. Sci.*, 1955, **42 A** (4), 175.

8. Iyengar, P. K. .. *J. Sci. Industr. Res.*, 1956, **15 A** (9), 399.

9. Glasstone, S. and Edlund, M. — *The Elements of Nuclear Reactor Theory*, 1952.

THE CHARACTERISTIC ROOTS OF THE PRODUCT OF MATRICES

By N. A. Khan

(*Muslim University, Aligarh*)

Received November 11, 1956
(Communicated by Dr. S. M. Shah, F.A.SC.)

1. Introduction

Let $A = (a_{rs})$ be an arbitrary square matrix of order n and $c(A)$ a characteristic root of A. Hirsch[5] proved that

$$| c(A) | \leq n \cdot \max_{1 \leq r,s \leq n} | a_{rs} |, \tag{1·1}$$

and Browne[3] obtained that

$$| c(A) | \leq (R + T)/2, \tag{1·2}$$

where

$$R = \max_{(r)} R_r = \max_{(r)} \sum_{\theta=1}^{n} | a_{rs} |, \quad T = \max_{(s)} T_s = \max_{(s)} \sum_{r=1}^{n} | a_{rs} |.$$

Further, Browne[2] showed that

$$s \leq | c(A) |^2 \leq G, \tag{1·3}$$

where s and G are the smallest and greatest characteristic roots of $A\bar{A}'$.

(1·1), (1·2) and other results established by several authors (for a list of references *see* [1]) give upper limits to $| c(A) |$ in terms of the elements of A, while (1·3) gives limits to $| c(A) |$ in terms of the characteristic roots of $A\bar{A}'$. In the present note an upper limit for $| c(A) |$ has been found in terms of the characteristic roots of the associated Hermitian matrices $(A + \bar{A}')/2$ and $(A - \bar{A}')/2i$, and this result has been generalised for the characteristic roots of the product matrix AB of two n-square real or complex matrices A and B. An upper limit for $| c(AB) |$ has also been found in terms of the elements of A and B. This result contains (1·2) as a particular case.

In establishing these results we use the well-known facts, *see* [4; p. 149], concerning the operator norm

$$\| A \| = \max. \| Ay \| \text{ for } \| y \| = 1, \text{ when } \| y \| = \sqrt{\bar{y}'y}.$$

In what follows $R(A) = \max_{(r)} R_r(A) = \max_{(r)} \sum_{s=1}^{n} |a_{rs}|$ and $T(A) = \max_{(s)} T_s(A) = \max_{(s)} \sum_{r=1}^{n} |a_{rs}|$.

2. Bound Theorem for $c(A)$

THEOREM 1.—*Let* $c(A)$ *be an arbitrary characteristic root of* A. *Then*

$$|c(A)| \leq \max. |c\left(\frac{A+\bar{A}'}{2}\right)| + \max. \left|c\left(\frac{A-\bar{A}'}{2i}\right)\right|. \qquad (2.1)$$

Proof.—Any square matrix $A = (A+\bar{A}')/2 + (A-\bar{A}')/2 = M + iN$, say, where M and N are Hermitian. Corresponding to an arbitrary characteristic root λ of A, there exists a non-zero column vector x, such that $\lambda x = Ax$. Then

$$\begin{aligned} |\lambda| \,.\, \|x\| = \|\lambda x\| &= \|Ax\| \\ &= \|(M+iN)\,x\| \\ &\leq \|M+iN\| \,.\, \|x\|, \end{aligned}$$

where for any square matrix B, $\|B\|^2 = \max_{\|y\|=1} \|By\| = \max_{\|y\|=1} (By, By)$ $= \max_{\|y\|=1} (\bar{y}'\bar{B}'By) = c_{\max.}(\bar{B}'B) = c_{\max.}(B\bar{B}')$, $c_{\max.}$ denoting the greatest characteristic root, and in particular if B is Hermitian $\|B\| = \max. |c(B)|$.

Since

$$\|x\| = \sqrt{\bar{x}'x} > 0,$$

we have

$$\begin{aligned} |\lambda| &\leq \|M+iN\| \\ &\leq \|M\| + \|N\| \\ &= \max. \left|c\left(\frac{A+\bar{A}'}{2}\right)\right| + \max. \left|c\left(\frac{A-\bar{A}'}{2i}\right)\right|. \end{aligned}$$

This establishes (2·1).

It may be observed that (1·3) and (2·1) give the same upper limit for $|c(A)|$ when A is Hermitian or skew-Hermitian. There are some other matrices also, for example $\begin{pmatrix} 1 & i \\ -3i & -1 \end{pmatrix}$, which are not of some special type but for which (1·3) and (2·1) give the same upper limit for $|c(A)|$. The limit for $|c(A)|$ given by (2·1) is not better than that given by (1·3), but,

in general, it is easier to find the characteristic roots of $(A + \bar{A}')/2$ and $(A - \bar{A}')/2i$ than those of $A\bar{A}'$.

3. BOUND THEOREMS FOR $c(AB)$

We now consider two theorems which give upper limits to the absolute value of an arbitrary characteristic root of the product matrix AB.

THEOREM 2.—*Let* $c(AB)$ *denote an arbitrary characteristic root of AB. Then*

$$|c(AB)| \leq \left[\max. \left|c\left(\frac{A+\bar{A}'}{2}\right)\right| + \max. \left|c\left(\frac{A-\bar{A}'}{2i}\right)\right|\right]$$

$$\times \left(\max. \left|c\left(\frac{\bar{B}+B'}{2}\right)\right| + \max. \left|c\left(\frac{\bar{B}-B'}{2i}\right)\right|\right). \tag{3.1}$$

Proof.—Any square matrix $A = (A + \bar{A}')/2 + (A - \bar{A}')/2 = M + iN$, say, and $B = (B + \bar{B}')/2 + (B - \bar{B}')/2 = R + iS$, say, where M, N, R and S are Hermitian matrices. Thus $AB = (M + iN)(R + iS)$.

If μ is an arbitrary characteristic root of AB, there exists a non-zero column vector x, such that $\mu x = ABx$ so that

$$\begin{aligned} |\mu| \, \|x\| &= \|\mu x\| \\ &= \|ABx\| \\ &\leq \|(M + iN)\| \, . \, \|(R + iS)\| \, . \, \|x\| . \end{aligned}$$

Since

$$\|x\| > 0,$$

we have

$$\begin{aligned} |\mu| &\leq \|M + iN\| \, . \, \|R + iS\| \\ &\leq (\|M\| + \|N\|)(\|R\| + \|S\|) \\ &= (\max. |c(M)| + \max. |c(N)|)(\max. |c(R)| \\ &\quad + \max. |c(S)|) \end{aligned}$$

since M, N, R and S are Hermitian matrices.

This establishes (3.1). It is easy to see that (3.1) can be generalised to the case of the product of any finite number of matrices $A_1, A_2, \ldots, A_k$ of the same order. The result in the generalised form is

$$|c(\prod_{r=1}^{k} A_r)| \leq \prod_{r=1}^{k} \left\{\max. \left|c\left(\frac{A_r+\bar{A}_r'}{2}\right)\right| + \max. \left|c\left(\frac{A_r-\bar{A}_r'}{2i}\right)\right|\right\}. \tag{3.2}$$

THEOREM 3.—*Let* $c(AB)$ *denote an arbitrary characteristic root of* AB. *Then*

$$|c(AB)| \leq \frac{R(A)+T(A)}{2} \cdot \frac{R(B)+T(B)}{2}. \tag{3.3}$$

Proof.—If μ is an arbitrary characteristic root of AB, there exists a non-zero column vector x, such that $\mu x = ABx$.

This gives, as we have seen in the proof of the previous theorem,

$$|\mu| \leq \|AB\| \leq \|A\| \cdot \|B\|$$
$$\leq \frac{R(A)+T(A)}{2} \cdot \frac{R(B)+T(B)}{2},$$

tor, by a known result [3; p. 708]

$$\|A\| = |c^{\frac{1}{2}}_{max.}(A\bar{A}')| \leq \frac{R(A)+T(A)}{2}.$$

This completes the proof of Theorem 3. It may be observed that (3.3) can be generalised to the case of the product of a finite number of matrices $A_1, A_2, \ldots\ldots A_k$ of the same order. The result in the generalised form is

$$|c(\overset{k}{\underset{r=1}{\Pi}} A_r)| \leq \overset{k}{\underset{r=1}{\Pi}} \frac{R(A_r)+T(A_r)}{2}. \tag{3.4}$$

4. PARTICULAR CASES OF THEOREM 3

(*i*) If we put $B = I$, (3.3) reduces to

$$|c(A)| \leq \frac{R(A)+T(A)}{2},$$

a result due to Browne,[3] quoted earlier.

(*ii*) If A and B are Hermitian or skew-Hermitian matrices, then $R_r(A) = T_r(A)$ and $R_r(B) = T_r(B)$ for $r = 1, 2, \ldots, n$, which means $R(A) = T(A)$ and $R(B) = T(B)$. Hence for Hermitian or skew-Hermitian matrices A and B

$$|c(AB)| \leq R(A)\,R(B). \tag{3.5}$$

In conclusion, I am thankful to Professor S. M. Shah for his help in the preparation of this paper.

REFERENCES

1. Brauer, A. .. "Limits for the characteristic roots of a matrix," *Duke Math. Journal*, 1946, **13**, 387–95.
2. Browne, E. T. .. "The characteristic equation of a matrix," *Bull. Amer. Math. Soc.*, 1928, **34**, 363–68.
3. ———— .. "The characteristic roots of a matrix," *Ibid.*, 1930, **36**, 705–10.
4. Halmos, P. R. .. *Finite Dimensional Vector Spaces*, Princeton, 1948.
5. Hirsch, A. .. "Sur les recines d'une equation fondamentale," *Acta Math.*, 1902, **25**, 367–70.

IMPROVEMENTS IN COLORIMETRIC DETERMINATIONS

III. Comparison of Colorimetric and Electrometric Methods for the Determination of Soil Reaction

By K. L. Khanna, F.A.Sc., P. B. Bhattacharya and K. Prasad

(*Central Sugarcane Research Station, Pusa, Bihar*)

Received October 29, 1956

I. Introduction

Mason and Obenstiain (1938) have, with proper manipulation, found that results obtained by Kuhn's (1930) colorimetric method of pH measurement agree closely with those of the electrometric method (1931). Errors in measurement may, however, occur through contamination, use of glassware of inferior quality and a high concentration of soluble salts in the soil. While carrying out pH determinations of a large number of samples collected from Narkatiaganj area (representing the non-calcareous soil division of North Bihar, with a low content of soluble salts), the authors had an opportunity of testing the colorimetric method against the standard electrometric method. The results of these studies have been reported in the present paper.

II. Experimental

The electrometric method.—10 grams of air-dry soil are taken with 25 c.c. of CO_2-free distilled water, stirred and examined in the Cambridge pH meter in the usual way.

Colorimetric method.—A layer of barium sulphate (Pro. Rontgen) 1 cm. thick is placed in the bottom of a dry test tube. A layer of soil about 3 cm. deep is then added and the tube filled with CO_2-free distilled water to a depth of 9 cm. Suitable indicator solutions depending upon the expected pH range are added and the test tube filled with water to a total depth of 15 cm. It is then closed with a paraffined cork, shaken vigorously for half a minute and left to settle. The colour developed is compared against Clarke's (1928) colour chart and the reading noted. The indicators used in the present case were Bromo Thymol Blue and Cresol Red prepared according to Clarke's procedure (*loc. cit*).

III. Discussion

The electrometric and colorimetric pH values of 300 samples were found to be in close agreement within a limit of 0·2 units in most cases. On

statistical examination of the data, the intra-class correlation coefficient worked out to 0·9879, indicating a very close agreement between the colorimetric and electrometric pH values. It may therefore be concluded that the colorimetric method may be employed satisfactorily in the estimation of pH in the field in case of soils with low soluble salt contents (below 150 mg./100 gm. soil) such as the non-calcareous soils of North Bihar (Prasad *et al.*, 1951).

IV. SUMMARY

pH values of 300 soil samples from Narkatiaganj area in North Bihar (non-calcareous soils with low soluble salt content) have been determined by the electrometric and colorimetric methods. The results are in close agreement, thus showing that the colorimetric method may be used for pH determinations in the field in case of soils of low soluble salt content.

V. ACKNOWLEDGEMENT

The work was carried out as part of the Sugarcane Research Scheme in Bihar being financed jointly by the Government of Bihar and the Indian Central Sugarcane Committee to whom grateful thanks are due. The assistance rendered by Sri. R. C. Acharya, M.A., Statistician, in statistically analysing the data is also acknowledged.

VI. REFERENCES

1. Clarke, W. M. .. *Hydrogen Ion Concentration*, W. & W. Company, U.S.A., 1928
2. Int. Soc. of Soil Science Soil Reaction Committee *Trans. 3rd Int. Cong. Soi. Sci.*, 1935, **1**, 127–32.
3. Kuhn, S. Z. .. *Pflans Dung.*, 193018A, 307–14.
4. Mason, D. D. and Obenstiain *Proc. Soil. Soc. Amer.*, 1938, **3**, 129–37.
5. Prasad, S. N., Bhattacharya, P. B. and Sinha, S. D. *Proc. First Bienn. Conf. Sugarcane Res. Workers, India*, 1951, 36–37.

POLAROGRAPHIC STUDIES ON THE COMPOSITION OF NICKEL FERROCYANIDE COMPLEX

By H. C. Saraswat and S. K. D. Agarwal

(Department of Chemistry, Christ Church College, Kanpur)

Received December 26, 1956

(Communicated by Prof. K. S. G. Doss, F.A.SC.)

Introduction

The composition of nickel ferrocyanide complex has been the subject of many investigations. Werner[1,2] studied for the first time the composition of nickel ferrocyanide complex and showed that Ni^{++} got precipitated with potassium ferrocyanide giving a stable complex of the composition Ni_2 [Fe $(CN)_6$]. Gaspar[3] and co-workers considered that the nickel ferrocyanide was a double complex or associated salt. Britton and Dodd[4] observed that nickel reacted with $K_4Fe(CN)_6$ to form normal salt which was converted by further precipitation into Ni_2 [Fe $(CN)_6$]. $x\,K_4$ [Fe $(CN)_6$], where x was less than one. Thermometric study[5] of precipitation of nickel ferrocyanide was shown to have a composition either NiK_2 [Fe $(CN)_6$] or Ni_4K_4 [Fe $(CN)_6]_3$, the composition varying with the conditions of precipitation. X-ray diffraction studies[6] of nickel ferrocyanide revealed that as much as 0·3–0·4 mole $K_4Fe(CN)_6$ existed with one molecule of Ni_2 [Fe $(CN)_6$]. It was assumed that the ferrocyanide was adsorbed on the surface of highly dispersed crystals of Ni_2 [Fe $(CN)_6$] and not combined to form definite double salts. The present communication reports polarographic investigation of the nickel ferrocyanide complex. This method appeared desirable: Potassium ferrocyanide is not reduced[7] at the d.m.e. and the method, therefore, is void of complications. Further, in a similar controversial circumstance, *viz.*, investigation of the composition of the cadmium ferrocyanide polarographic method proved to be successful.[8]

Experimental

Nickel sulphate used was B.D.H. Analar sample. This was recrystallised in twice distilled water and dried at 50° C. for 48 hours. The exact concentration of the nickel solution prepared was estimated gravimetrically using dimethyl glyoxime.

Potassium ferrocyanide used was Merck sample. KCl employed was of B.D.H. Analar quality.

The polarograph used was assembled in our Laboratory; the electrical circuit employed was similar to the one described in an earlier communica-

tion.[9] The diffusion current was obtained by measuring the potential difference developed across a known resistance introduced serially in the circuit; the accuracy of the measurement was adjusted to $0 \cdot 1\ \mu$ amp.

The capillary employed had the following characteristics:

$$m = 0 \cdot 665 \text{ mgm./sec.}$$

$$t = 4 \cdot 14 \text{ sec.}$$

These values were recorded in 0·1 M KCl solution in open circuit.

The method employed for investigating the nickel ferrocyanide complex involved the amperometric titration of a known volume of Ni^{++} solution of a fixed strength against standard potassium ferrocyanide. 1 M KCl solution was used as supporting electrolyte and 0·02 per cent. solution of gelatin was used as the maximum suppressor. The titrations were carried out at $-1 \cdot 9$ volts where the diffusion current attained a limiting value; and in an inert atmosphere of nitrogen to avoid the possible oxidation of nickel ferrocyanide complex,[10] leading to a change in colour of the precipitate from green to yellowish brown; it may be added that in the present studies no such change in the colour has been noticed.

RESULTS AND DISCUSSION

Figure 1 gives a typical series of results on the variation of diffusion current during the progress of the amperometric titration of Ni^{++} with $K_4Fe(CN)_6$ in presence of 1 M KCl used as supporting electrolyte. The data in Fig. 1 show that sharp end points could be obtained during the

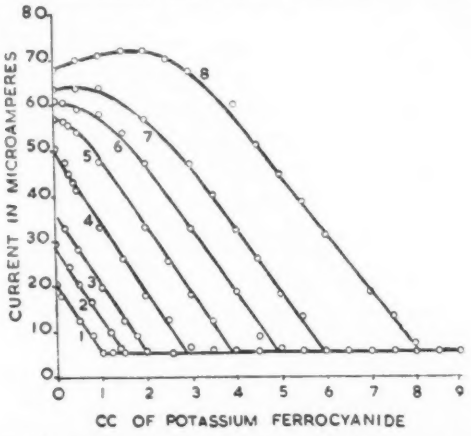

FIG. 1. Amperometric titration of Ni against potassium ferrocynide.

Concentration of ferrocynide 100 mM. Curves 1 to 8 refer respectively to 5, 7·5, 10·0, 15·0, 20·0, 25·0, 30·0, 40·0 millimolar of Ni^{++}, applied voltage $-1 \cdot 9$ volts.

titration of Ni^{++} with ferrocyanide polarographically. The observed quantities of potassium ferrocyanide for different concentrations of Ni^{++} are given in Table I. It is interesting to note from the data in columns 3 and 4 (Table I) that the composition of nickel ferrocyanide complex corresponded to Ni_5K_6 [Fe $(CN_6]_4$; this appears to follow the stoicheometric relationship according to the equation

$$5\ NiSO_4 + 4\ K_4Fe\ (CN)_6 \rightarrow Ni_5K_6\ [Fe\ (CN)_6]_4 + 5\ K_2SO_4.$$

TABLE I

Polarographic investigation of nickel ferrocyanide complex

Volume of Ni^{++} solution in the cell 25·00 ml.

Concentration of Ni^{++} solution in mM (1)	Concentration of $K_4Fe\ (CN)_6$ in mM (2)	Observed titre value in ml. (3)	Volume required on the basis of the formula $Ni_5K_6[Fe(CN)_6]_4$ (4)
1·25	50	0·5	0·5
2·5	50	1·0	1·0
5·0	50	2·05	2·0
7·5	50	3·0	3·0
10·0	50	4·0	4·0
12·5	50	5·0	5·0
15·0	50	6·05	6·0
17·5	50	7·0	7·0
20·0	50	8·0	8·0
25·0	50	10·05	10·0
30·0	50	12·0	12·0
40·0	50	16·05	16·0
5·0	100	1·0	1·0
7·5	100	1·45	1·5
10·0	100	2·0	2·0
15·0	100	3·0	3·0
20·0	100	4·0	4·0
25·0	100	5·0	5·0
30·0	100	6·05	6·0
40·0	100	8·0	8·0

The results showed conclusively that over a wide range of concentration of Ni^{++} and $K_4Fe\ (CN)_6$, the composition of the complex, as derived from the end points of amperometric titration curves, appeared to be Ni_5K_6 [Fe $(CN)_6]_4$ or 3 NiK_2 [Fe $(CN)_6$], Ni_2 [Fe $(CN)_6$].

The data further show that the method could be employed with ease for quantitative estimation of Ni^{++}. The experimental error involved is less than 1 per cent.

A detailed examination of the titration curves shows a significant feature in the variation of the diffusion current at the initial stages of the titration. While the diffusion current was expected to decrease continuously with the addition of the titrant leading to the familiar *L*-shaped curves, in the present investigation the current values did not decrease in the initial stages and remained almost unaffected; this feature was more apparent at higher concentrations of nickel; in fact the current values increased (*see* curves 6–8, Fig. 1). Extrapolation of the straight line portion of the curves to Y-axis indicated that initial values of the limiting current should be much greater than the observed values.

The following Ilkovic's equation gives the theoretical values of limiting current i_d for different concentration of an electro-active substance:

$$i_d = 605\ nCD^{\frac{1}{2}}\ m^{\frac{2}{3}}t^{\frac{1}{6}}$$

where C is the concentration of the substance in millimolars; n, the number of electrons involved in the electrode reaction; D, the diffusion coefficient of the ion in $cm.^2\ sec.^{-1}$; m, the rate of flow of mercury in mgm./sec.; and t, the time in secs. for 1 drop of mercury flowing through the capillary. Table II gives the observed values and the values of i_d calculated from the above equation for different concentrations of Ni^{++}; in these,

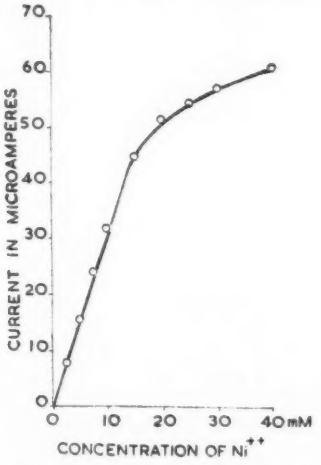

FIG. 2. Variation of the limiting current with the concentration of Ni^{++}.

D has been taken as $0{\cdot}69 \times 10^{-5}$ cm.^{2}/sec.[11] The data in Table II show clearly that the i_d values do not follow Ilkovic's equation above 15 mM. concentration (*see* also Fig. 2). It is interesting to note from these data that

TABLE II

Applicability of Ilkovic's equation to the limiting current of Ni^{++}

Concentration of Ni^{++} in mM. (1)	i_d calculated from Ilkovic's equation in μ amps. (2)	i_d observed in μ amps. (3)	Deviation per cent. (4)
2·5	7·67	7·7	1·0
5·0	15·35	15·3	0·3
7·5	20·02	24·1	4·6
10·0	30·7	31·8	3·5
15·0	46·05	44·3	3·8
20·0	61·4	51·5 (61·0)	16·1
25·0	76·75	54·9 (75·0)	29·8
30·0	92·1	57·4 (90·0)	37·6
40·0	122·8	61·1 (117·0)	50·2

The values of i_d given in the paranthesis refer to those obtained by extrapolation of straight line portion of amperometric curves to the Y-axis (*see* Fig. 1).

the peculiar behaviour of the amperometric titration curves, *viz.*, the non-linear variation of the current in initial stages of the titration, is closely associated with the non-applicability of Ilkovic's equation at higher concentrations. Since, however, the end points even at these high concentrations were very sharp, Ni^{++} could be estimated polarographically upto 40 mM. concentration using $K_4Fe(CN)_6$ as the titrant.

SUMMARY

The composition of nickel ferrocyanide was investigated following the amperometric titration of Ni^{++} up to 40 mM. concentration against potassium ferrocyanide; it appeared to be $3\ NiK_2\ [Fe\ (CN)_6]$, $Ni_2\ [Fe\ (CN)_6]$ or $Ni_5K_6\ [Fe\ (CN)_6]_4$. The data showed the possibility of estimating Ni^{++} polarographically within an experimental error of 1 per cent.

ACKNOWLEDGEMENTS

Authors' thanks are due to Dr. N. A. Ramaiah, Head of the Department of Physical Chemistry, Indian Institute of Sugar Technology, Kanpur, for suggesting the problem and helpful discussion during the progress of the work, and to Revd. R. G. Slater, M.A. (Cantab), Principal, Christ Church College, for his kind interest.

REFERENCES

1. Werner .. *Pharm. Zty.*, 1918, **55**, 211–12.
2. ———— .. *Z. anal. Chem.*, 1919, **58**, 23–24.
3. Gaspar, Arnal and Alberto Castro, Girona Y. Pozurama — *Anales Soc. espan. fis. quim.*, 1926, **24**, 323–35.
4. Britton and Eric N. Dodd — *J. Chem. Soc.*, 1933, 1543–46.
5. Rene Paris .. *Compt. rend.*, 1934, **199**, 863–65.
6. Harry, Weiser, Milligan and Bates — *J. Phys. Chem.*, 1938, **42**, 945–54.
7. Sanigar, G. .. *Trav. Chim. Pays. Bas.*, 1925, **44**, 59.
8. Ramaiah and Agarwal .. *Proc. Ind. Acad. Sci.*, 1956, **44 A**, 134.
9. ———— .. *Ibid.*, 1956, **44 A**, 26.
10. Nilsson .. *Chem. Zentr.*, 1942, **1**, 2972.
11. Kolthoff and Lingane .. *Polarography*, Interscience Publication, Inc., New York, 1952, **1**.

CHROMATOGRAPHIC STUDIES ON THE KINETICS OF THE PRODUCTION OF CARAMEL

By N. A. Ramaiah, S. K. D. Agarwal and J. K. P. Agarwal
(Department of Physical Chemistry, Indian Institute of Sugar Technology, Kanpur)

Received December 14, 1956
(Communicated by Prof. S. N. Gundu Rao, F.A.SC.)

Caramel is a mixture of nitrogen-free organic compounds and is one of the colouring matters that are produced during the manufacture of cane sugar, chiefly due to overheating of sugars.[1] Caramel not only affects the colour of sugar but also retards crystallisation.[2] It is manufactured on a large scale for purposes of colouring liquors, sweetmeats and gravies.[3,4]

There are three main components in cane juice which are responsible for the production of caramel during the manufacture of cane sugar: these are sucrose, glucose and fructose. The process of conversion of sucrose into caramel acquires appreciable velocity only at pH $\geq$ 9,[5] while in the manufacture of cane sugar, the different processes are operated, after the initial purification of the juice, nearly at neutral pH. Cane juice contains 0·5 to 2 per cent. of a mixture of glucose and fructose; these have been found to be the most important sources for the production of the colouring matter during sugar manufacture.[6] The production of caramel from glucose has been studied by Geils,[7] while the same from fructose has been examined by Ripp[8] and others.

The exact chemical composition of caramel is not yet available. Schumaker and Buchanan[9] reported that when solid sucrose was heated at about 200° C., three periods of foaming occurred, indicating the splitting of water at each stage and resulting in the formation of anhydrides with the empirical formulæ, $C_{12}H_{20}O_{10}$, $C_{24}H_{36}O_{18}$ and $C_{36}H_{50}O_{25}$. Recently, Luckesch[10] chromatographically analysed caramel prepared from sucrose and reported that it contained glucose, fructose, glyceryl aldehyde, dihydroxy acetone, pyruvic acid, hydroxy methyl furfural and methyl glyoxal. Authors' chromatographic studies[11] of the caramels prepared by heating glucose, fructose, maltose, sucrose and liquid glucose, in alkaline solutions, indicated the presence of four reducing compounds constituting caramel, with the following R_f ($\times$ 100) values: 0, 1·4, 4·4 and 6·5 (standard reference value = levulose — 13·6). The observation of a spot on the reference line on the chromatogram (R_f value = 0), which could not be separated from the base line even by running the chromatogram for more than 5 days, indicated

the presence of one or more reducing compounds of very large molecular weight.[11] Authors' chromatographic analysis indicated the presence of no acids in the caramels.

Although attempts as mentioned above have been made to elucidate the composition of caramel, very few investigations seem to have been undertaken to study the kinetics or the mechanism of the production of caramel. The present communication reports data on chromatographic studies on the kinetics of the production of caramel from glucose.

§ 2. EARLIER WORK

The first attempt to investigate the kinetics of the development of colour in sugar solutions seems to have been made by Doss and Ghosh.[12] These authors employed a spectro-photometer (Spekker) and studied the time development of colour in the invert sugar in alkaline solutions; they observed that "double the concentration of invert sugar in the reaction mixture nearly doubled the rate of colour development"; and inferred, therefore, that the colour development in alkaline solutions at ordinary temperatures is essentially of the first order. The present authors[13] also studied spectrophotometrically (using Unicam S.P. 350 D.G. spectrophotometer) the development of colour in alkaline glucose solutions, at different temperatures in the range 35°–70° C.; and found that the following equation was applicable to the data on the time development of the colour in glucose at temperatures greater than 50° C.:

$$a - r = ae^{-kt}$$

where a is the total initial concentration of the substance undergoing change or the value of the optical density proportional to the concentration thereof; r, the amount decomposed upto time t; and k, the characteristic velocity constant of a first order reaction. This observation suggested that the production of colour or caramel from glucose, when heated in alkaline solutions at temperatures above 50° C., is first order in nature. Employing the familiar Arhenius equation, the apparent energy of activation of the process involved has been computed from the data obtained at different temperatures; an average value of this appeared to be 11·9 kcal.

An interesting observation recorded by the present authors[13] and also by Doss and Ghosh,[12] was that the initial portion of the curves representing the variation of the optical density with time was concave in shape towards the X-axis (*see* Figs. 1 and 2); this feature is clearly seen from the data obtained at low temperatures, say 40° C. (*see* Curve 1, Fig. 2). At higher temperatures the concavity is noticeable only at very low time intervals.

§ 3. Present Investigation

The data in Figs. 1 and 2, especially the observed concavity towards X-axis of the optical density — time curves, suggested the following two important deductions[13]:

Fig. 1.

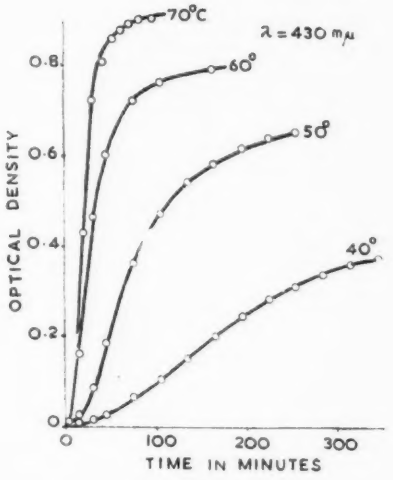

Fig. 2.

Fig. 1. Variation of the optical density with time during caramelisation of invert sugar (*cf.* Ref. 12).

Fig. 2. Variation of the optical density with time during caramelisation of glucose at different temperatures (*cf.* Ref. 13).

(*i*) the substance or one of the substances produced initially aids or catalyses the decomposition of glucose into different substances composing the caramel; or/and

(*ii*) the substance or substances produced initially undergo further reaction presumably obeying a first order law, to give the final products; that is, the conversion of glucose into caramel is apparently through the formation of intermediate compound(s).

These deductions have now been examined, in some detail, employing the filter paper chromatographic technique. The procedure involved the chromatographic investigation of the reaction mixture at different intervals of time during the progress of the reaction.

§ 4. Experimental

Analar samples of glucose and sodium hydroxide were used. Known quantities of solutions of these substances, of desired strength, were mixed

together such that the final solution was of a pH value in the range 10–13. About 100 c.c. of the mixed solution was taken into a glass vessel which was immersed in a paraffiin oil thermostat. The temperature of this last could be raised to and maintained constant ($\pm 0{\cdot}1°$) at any desired value.

During the development of colour in the alkaline glucose solutions at a fixed temperature, a small quantity of the reaction mixture was withdrawn at regular intervals of time and was used for chromatographic analysis. It is to be pointed out that the portion of the reaction mixture withdrawn for analysis was quickly cooled to the room temperature and thus the progress of the reaction in the sample got practically quenched.

The method employed for chromatographic analysis was essentially the same as used by Patridge.[11] Strips, of suitable width, of Whatman filter paper No. 1, were used. The reaction mixture under examination was spotted on a (reference) line drawn parallel to one edge of the filter paper strip. The solvent used was the top layer of a mixture of butanol, ethanol and water (50 : 10 : 40 by volume). The bottom layer was used for saturating the chamber in which the filter paper strips were suspended. After the chromatograms were run for 70–100 hrs., they were dried and washed with a solution of silver nitrate in acetone. They were later dried again and sprayed with alcoholic KOH solution, when brown or dark brown spots referring to the reducing compounds present in the reaction mixture, became apparent. The chromatograms were later treated with ammonia, washed with continuous flow of water for 2 hrs. and finally dried.

§ 5. RESULTS

Figures 3 and 4 refer to two typical chromatograms. These refer to reaction mixtures drawn at regular intervals from the reaction vessel in which

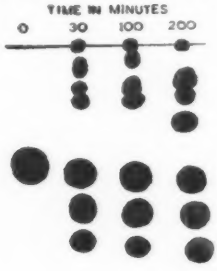

FIG. 3.

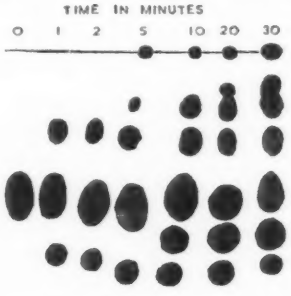

FIG. 4.

FIG. 3. Chromatographic studies of the composition of the reaction mixture at different time intervals during caramelisation of glucose at 40° C.

FIG. 4. Chromatographic studies of the composition of the reaction mixture at different time intervals during caramelisation of glucose at 70° C.

glucose has been heated with alkali solution at 40° and 70° C. respectively. The running time for the chromatograms of Fig. 4 was 72 hrs., while the same for the others given in Fig. 3 was 90 hrs. The R_f values for the spots observed in Figs. 3 and 4 are returned in Table I; these were computed by comparison of the spots developed for known sugars in a previous run on a separate strip of filter paper.

TABLE I

R_f values of the spots observed in the chromatographic studies on the kinetics of caramel formation

Spot No.	Time in Minutes			
	0	30	100	200
	Temperature of Reaction Vessel = 40° C.			
1		0	0	0
2		2·1	2·1	2·8
3		4·5	4·5	4·3
4				6·5
5	9·5	9·5	9·5	9·5
6		12·8	12·9	13·0
7		14·9	15·0	15·0

	0	1	2	5	10	20	30
	Temperature of Reaction Vessel = 70° C.						
1				0	0	0	0
2						2·8	2·8
3				4·3	4·4	4·4	4·4
4		7·8	7·8	7·8	7·8	7·8	7·8
5	9·5	9·5	9·5	9·5	9·5	9·5	9·5
6		12·8	12·8		12·2	12·2	12·2
7				14·2	14·2	14·2	14·0

The chromatograms taken with the reaction mixture obtained in the beginning of the reaction, *i.e.*, at zero interval of time, indicated the presence of only one spot corresponding to glucose [with an R_f ($\times$ 100) value of 9·5]. The chromatograms referring to the reaction mixture drawn at increasing intervals of time, showed spots other than that of glucose. It was interesting to note that the reaction mixture obtained at 2 mts. intervals of time contained, as indicated by chromatographic analysis (Fig. 4), three compounds, excluding glucose, the R_f ($\times$ 100) values of these are approximately as follows: 3·0, 4·1 and 12. The production of a compound with an R_f value of 12 referring to fructose (R_f value 13 was particularly instructive in light of the finding due to Lobry de Bruyn and van Ekenstein[15] who showed that during heating of sugars in alkaline solutions for caramelisation, equilibrium mixture of glucose and fructose (as also mannose) are produced; in accord with this is the observation of the authors[11] that whatever may be the sugar employed initially for caramelisation, the same reducing compounds have been detected in chromatographic analysis of the caramels. Further, the data in Figs. 3 and 4 show that the spaces where the original mixture was placed on the reference line for chromatographic analysis, acquired colour only after 25 mts. in the reaction mixture maintained at 40° C. (Fig. 3) and 2 mts. interval of time in the reaction mixture maintained at 70° C. (Fig. 4). This spot (R_f value = 0) on the reference line, which could not be separated from this last even by running the chromatogram for 5 or 6 days indicated, as mentioned above (§ 1), the presence of reducing substance(s) of high molecular weight. This observation suggests that the substances composing caramel are produced after the initial generation of certain substances with low molecular weight.

§ 6. DISCUSSION

The following is the resume of the important findings on the kinetics of the production of caramel:

(*i*) During heating of glucose and other sugars in alkaline solutions, compounds of low molecular weight are produced initially,

(*ii*) Lobry de Bruyn and van Ekenstein transformation takes place;

(*iii*) the production of caramel involves autocatalysis; and

(*iv*) the reaction involves a step which controls the time development of colour and which obeys a first order law.

These observations lead the authors to suggest the following mechanisms:

(*A*) Heating of glucose or other sugars in alkaline olutions, leads to the initial production of an equilibrium mixture of glucose, fructose and

mannose; these apparently condense together to form an intermediate compound of very high molecular weight, which decomposes unimolecularly to yield the compounds [with R_f ($\times$ 100) values 0, 1·3, 4·4 and 6·6, in reference to levulose — 13·6] constituting caramel, one of which acts as a catalyst to the establishment of Lobry de Bruyn and van Ekenstein transformation.

(*B*) Alternatively, the rate determining step in the process is likely to be the establishment of Lobry de Bruyn and van Ekenstein transformation and the autocatalytic nature is related to the decomposition of the condensation product contemplated in (*A*).

The observation of the autocatalytic nature of the reaction upto 30 mts. at 40° C. and upto 2 mts. at 70° C. suggests that the mechanism (*A*) is to be preferred. Conclusive evidence is, however, lacking.

§ 7. Summary

The kinetics of production of caramel which is a mixture of nitrogen-free organic compounds and which offers colour to sugar crystals and retards the rate of crystallisation, have been investigated by employing filter paper chromatographic technique. Chromatograms of the reaction mixture, *viz.*, glucose heated in alkaline solutions, at different intervals of time during the progress of the reaction showed the initial production of compounds of low molecular weight, which condensed to form an intermediate compound of very high molecular weight; this last appeared to decompose unimolecularly to give the products composing caramel.

§ 8. Acknowledgement

Authors' thanks are due to Professor S. N. Gundu Rao, B.Sc., A.H.B.T.I., F.R.I.C., F.A.Sc., Director and to Professor K. S. G. Doss, D.Sc., F.R.I.C., F.Inst.P., F.A.Sc., Professor of Sugar Chemistry, Indian Institute of Sugar Technology, Kanpur, for their kind interest and encouragement during the work; and to the Ministry of Education, Government of India, for a Fellowship to one of us (S.K.D.A.).

References

1. Zerban .. *Techn. Repts., Sugar Res. Foundation*, No. 2, 1947, 1.
2. Dass and Ghosh .. *Proc. Sugar Tech. Assocn.*, 1951, **19**, 183.
3. .. *Manufacture of Confectionery*, Iudustry Publishers, Fifth Edition.
4. Jordan .. *Confectionery Standards*, Applied Sugar Laboratories, N.Y., 1933.

5.	Spengler, Bottger and Seeliger		*Zeit. Wirtschaftsgruppe Zuckerind*, 1936, **86,** 193.
6.		..	*Cf. ref.* **1**, p. 3.
7.	Geils	..	*Compt. rend.*, 1857, **45,** 590.
8.	Ripp	..	*Zeit. Ver. dent. Zuckerind*, 1925, **75,** 635.
9.	Schumaker and Buchanan		*Iowa State Coll. Jour. Sci.*, 1932, **6,** 367.
10.	Lukesch	..	*Naturwiss.*, 1955, **43,** 108.
11.	Ramaiah, Agarwal and Agarwal		*Curr. Sci.*, in proof.
12.	Doss and Ghosh	..	*Proc. Sugar. Tech. Assocn.*, 19, **17,** 51; 19, **18,** 26.
13.	Ramaiah, Agarwal and Agarwal		*Ibid.*, 1956, **24,** 69.
14.	Patridge	..	*Nature*, 1946, **158,** 270.
15.	Lobry de Bruyn and van Ekenstein		*Rev. trav. Chim.*, 1895, **14,** 156; 1897, **16,** 253.

NEW SOLUTIONS FOR FINITE DEFORMATION

By B. R. Seth, F.A.Sc.

(*Kharagpur*)

Received January 10, 1957

1. Introduction

In recent years the theory of finite deformation has received fresh impetus from a number of exact solutions that have been obtained for imcompressible elastic bodies without assuming any form of the strain energy function. The exact solutions obtained for compressible bodies have not been very large, and in general they have been of the form obtained by B. R. Seth. Extensive references to existing literature on the subject are given in the Presidential Address to the Section of Mathematics at the 42nd Session of the Indian Science Congress.[1]

Very few attempts have been made to obtain solutions for the finite bending of plates into shells. The earliest exact solution on the basis of a linear stress strain tensor law was obtained by Seth[2] for a rectangular plate bent into a right cylindrical shell. The form of this solution has been used by many workers. In the present paper an attempt has been made to discuss solutions which may be used to discuss the finite bending of plates into spherical shells. A linear stress strain tensor law is again assumed, and this gives sufficiently good results for technical applications.

In cylindrical co-ordinates it is found that, if we take

$$u = r - \phi(r, z), \quad v = \theta - A\theta, \quad w = z - f(r^2 + z^2),$$

all the equations of finite deformation and boundary conditions on a spherical shell can be satisfied only if

$$\phi = \alpha r, \quad f(r^2 + z^2) = -\frac{2c_1}{1-c}(r^2 + z^2)^{\frac{1}{2}(1-c)},$$

where α, A, c_1 are known constants and $c = (1 - 2\sigma)/(1 - \sigma)$ is an elastic constant.

2. Finite Strain Components in Cylindrical Co-ordinates

For all applications finite strain components should be referred to the strained state of the body. Let ${}^{i}x$ be the unstrained and x^i the strained co-ordinates of the deformed body with reference to a fixed frame with ${}_{ij}g$ and g_{ij} as metric tensors. The strain tensor e_{ij} is given by[3]

$$2\epsilon_{ij} = g_{ij} - {}_{\alpha\beta}g\,({}^{\alpha}x_{,i})\,({}^{\beta}x_{,j}). \tag{2.1}$$

Putting $u^i = x^i - {}^ix$, (2.1) becomes

$$2\epsilon_{ij} = g_{ij} - {}_{ij}g + {}_{\alpha j}g u^{\alpha}{}_{,i} + {}_{i\beta}g u^{\beta}{}_{,j} - {}_{\alpha\beta}g u^{\alpha}{}_{,i}\, u^{\beta}{}_{,j}. \tag{2.2}$$

In cylindrical co-ordinates

$$\begin{gathered} {}^ix = r_0,\ \theta_0,\ z_0,\ \ x^i = r,\ \theta,\ z, \\ u = r - r_0,\ \ v = \theta - \theta_0,\ \ w = z - z_0, \\ {}_{ij}g = \begin{bmatrix} 1 & 0 & 0 \\ 0 & r_0{}^2 & 0 \\ 0 & 0 & 1 \end{bmatrix}, g_{ij} = \begin{bmatrix} 1 & 0 & 0 \\ 0 & r^2 & 0 \\ 0 & 0 & 1 \end{bmatrix}. \end{gathered} \tag{2.3}$$

The tensor components ϵ_{ij} can be replaced by the physical components e_{ij} by the relation[4]

$$e_{ij} = (g^{ii}g^{jj})^{\frac{1}{2}}\epsilon_{ij}. \tag{2.4}$$

Thus we get the components of finite strain in cylindrical co-ordinates as[5]

$$\begin{aligned} 2e_{rr} &= 2\frac{\partial u}{\partial r} - \left[\left(\frac{\partial u}{\partial r}\right)^2 + r^2\left(\frac{\partial v}{\partial r}\right)^2 + \left(\frac{\partial w}{\partial r}\right)^2\right] \\ &\quad + 2ru\left(\frac{\partial v}{\partial r}\right)^2 - u^2\left(\frac{\partial v}{\partial r}\right)^2, \\ 2e_{\theta\theta} &= 2\frac{u}{r} + 2\frac{\partial v}{\partial \theta} - \frac{u^2}{r^2} - 4\frac{u}{r}\frac{\partial v}{\partial \theta} \\ &\quad - \left[\frac{1}{r^2}\left(\frac{\partial u}{\partial \theta}\right)^2 + \left(\frac{\partial v}{\partial \theta}\right)^2 + \frac{1}{r^2}\left(\frac{\partial w}{\partial \theta}\right)^2\right] \\ &\quad + 2\frac{u^2}{r^2}\frac{\partial v}{\partial \theta} - 2\frac{u}{r}\left(\frac{\partial v}{\partial \theta}\right)^2 + \frac{u^2}{r^2}\left(\frac{\partial v}{\partial \theta}\right)^2, \\ 2e_{zz} &= 2\frac{\partial w}{\partial z} - \left[\left(\frac{\partial u}{\partial z}\right)^2 + r^2\left(\frac{\partial v}{\partial z}\right)^2 + \left(\frac{\partial w}{\partial z}\right)^2\right] \\ &\quad + 2ru\left(\frac{\partial v}{\partial z}\right)^2 - u^2\left(\frac{\partial v}{\partial z}\right)^2, \end{aligned}$$

$$2e_{\theta z} = \frac{1}{r}\frac{\partial w}{\partial \theta} + r\frac{\partial v}{\partial z} - 2u\frac{\partial v}{\partial z}$$

$$- \left[\frac{1}{r}\frac{\partial u}{\partial \theta}\frac{\partial u}{\partial z} + r\frac{\partial v}{\partial \theta}\frac{\partial v}{\partial z} + \frac{1}{r}\frac{\partial w}{\partial \theta}\frac{\partial w}{\partial z}\right]$$

$$- \frac{u^2}{r^2}\frac{\partial v}{\partial \theta} + 2u\frac{\partial v}{\partial \theta}\frac{\partial v}{\partial z} - \frac{u^2}{r}\frac{\partial v}{\partial \theta}\frac{\partial v}{\partial z},$$

$$2e_{zr} = \frac{\partial u}{\partial z} + \frac{\partial w}{\partial r} - \left[\frac{\partial u}{\partial z}\frac{\partial u}{\partial r} + r^2\frac{\partial v}{\partial z}\frac{\partial v}{\partial r} + \frac{\partial w}{\partial z}\frac{\partial w}{\partial r}\right]$$

$$+ 2ru\frac{\partial v}{\partial z}\frac{\partial v}{\partial r} - u^2\frac{\partial v}{\partial z}\frac{\partial v}{\partial r},$$

$$2e_{r\theta} = r\frac{\partial v}{\partial r} + \frac{1}{r}\frac{\partial u}{\partial r} - 2u\frac{\partial v}{\partial r}$$

$$- \frac{1}{r}\left[\frac{\partial u}{\partial r}\frac{\partial u}{\partial \theta} + r\frac{\partial v}{\partial r}\frac{\partial v}{\partial \theta} + \frac{1}{r}\frac{\partial w}{\partial r}\frac{\partial w}{\partial \theta}\right]$$

$$+ \frac{u^2}{r}\frac{\partial v}{\partial r} + 2u\frac{\partial v}{\partial r}\frac{\partial v}{\partial \theta} - \frac{u^2}{r}\frac{\partial v}{\partial r}\frac{\partial v}{\partial \theta}. \qquad (2.5)$$

We have now to use the semi-inverse method of assuming a possible set of displacements. For the type of problem in view we should take

$$u = r - \phi(r, z),\ v = \theta - \mathrm{A}\theta,\ w = z - f(r^2 + z^2), \qquad (2.6)$$

where f and ϕ are arbitrary functions to be determined and A is a constant. The corresponding strain components are found to be

$$e_{rr} = \tfrac{1}{2}(1 - \phi_r{}^2) - 2r^2 f'^2,\ e_{\theta\theta} = \mathrm{K}_0 - \tfrac{1}{2}\mathrm{K}\frac{\phi^2}{r^2},$$

$$e_{zz} = \tfrac{1}{2}(1 - \phi_z{}^2 - 4z^2 f'^2),\ e_{rz} = -\tfrac{1}{2}(\phi_r\phi_z + 4rzf'^2),$$

$$e_{\theta z} = 0,\quad e_{r\theta} = 0, \qquad (2.7)$$

where

$$\mathrm{K}_0 = \tfrac{1}{2} - (1 - \mathrm{A})^2,\quad \mathrm{K}_1 = 1 - 2(1 - \mathrm{A}) - (1 - \mathrm{A})^2, \qquad (2.8)$$

$$\phi_r = \frac{\partial \phi}{\partial r},\ \phi_z = \frac{\partial \phi}{\partial z},\ f' = \frac{\partial f}{\partial \mathrm{R}^2},\ \mathrm{R}^2 = r^2 + z^2.$$

3. STRESS-STRAIN RELATIONS AND BODY-STRESS EQUATIONS

We assume that

$$\tau_{ij} = \lambda\delta_{ij}\Delta + 2\mu e_{ij}. \tag{3.1}$$

The body-stress equations of equilibrium are

$$\tau_{ij,\,j} = 0, \tag{3.2}$$

and

$$\Delta = 1 - K_0 - 2(r^2 + z^2)f'^2 - \tfrac{1}{2}K_1\frac{\phi^2}{r^2} - \tfrac{1}{2}(\phi_r{}^2 + \phi_z{}^2). \tag{3.3}$$

Substituting the value of e_{ij} from (2.7) we see that the first equation gives

$$\frac{\partial}{\partial r}[\lambda\Delta - 8\mu\int f'^2 dR^2 - 8\mu\int R^2 f'f''dR^2 - \mu(\phi_r{}^2 + \phi_z{}^2)]$$

$$+\frac{\mu}{r}\left(1 - 2K_0 + K_1\frac{\phi^2}{r^2}\right) - \mu\phi_r{}^2\left[\frac{\partial}{\partial z}\left(\frac{\phi_z}{\phi_r}\right) + \frac{1}{r}\right] = 0. \tag{3.4}$$

The second is identically satisfied and the third gives

$$\frac{\partial}{\partial z}[\lambda\Delta - 8\mu\int f'^2 dR^2 - 8\mu\int R^2 f'f''dR^2 - \mu(\phi_r{}^2 + \phi_z{}^2)]$$

$$+\mu\phi_r{}^2\left[\frac{\partial}{\partial r}\left(\frac{\phi_z}{\phi_r}\right) - \frac{1}{r}\frac{\phi_z}{\phi_r}\right] = 0. \tag{3.5}$$

These will be satisfied by

$$P \equiv \lambda\Delta - 8\mu\int f'^2 dR^2 - 8\mu\int R^2 f'f''dR^2 - \mu(\phi_r{}^2 + \phi_z{}^2)$$

$$= a \text{ constant}, \qquad R^2 = r^2 + z^2. \tag{3.6}$$

provided

$$\frac{\partial}{\partial r}\left(\frac{\phi_z}{\phi_r}\right) - \frac{1}{r}\frac{\phi_z}{\phi_r} = 0. \tag{3.7}$$

$$\frac{1}{r}\left(1 - 2K_0 + \frac{K_1\phi^2}{r^2}\right) - \phi_r{}^2\left[\frac{\partial}{\partial z}\left(\frac{\phi_z}{\phi_r}\right) + \frac{1}{r}\right] = 0. \tag{3.8}$$

From (3.7) we get

$$\frac{\phi_z}{\phi_r} = r\chi'(z), \tag{3.9}$$

which gives

$$\phi = F[\chi(z) + \log r], \tag{3.10}$$

where χ and F are arbitrary functions of z and $\chi(z) + \log r$ respectively. Substituting this value of ϕ in (3.8) we get

$$(1 - 2K_0)\, r^2 + K_1F^2 - r^2F'^2\chi''(z) - F'^2 = 0. \tag{3.11}$$

From (3.6) we see that

$$\tfrac{1}{2}\lambda K_1 \frac{\phi^2}{r^2} + (\tfrac{1}{2}\lambda + \mu)(\phi_r{}^2 + \phi_z{}^2) = M(r^2 + z^2), \tag{3.12}$$

M being an arbitrary function of $(r^2 + z^2)$. Substituting from (3.10) we get

$$K_1F^2 + \frac{\lambda + 2\mu}{\lambda}\left[r^2F'^2\chi'^2(z) + F'^2\right] = \frac{2r^2M}{\lambda}. \tag{3.13}$$

Comparing (3.11) with (3.13) we get

$$\left.\begin{aligned} M &= -\tfrac{1}{2}\lambda(1 - 2K_0) \\ \chi'' &= \chi'^2, \end{aligned}\right\} \tag{3.14}$$

Thus

$$\chi = -\log(cz + D),$$

and

$$\phi = F\left[\log \frac{r}{cz + D}\right]. \tag{3.15}$$

Also

$$\left[\frac{r^2c^2}{(cz + D)^2} + 1\right] F'^2 = (1 - 2K_0)\, r^2 + K_1F^2,$$

which shows that $c = 0$ and

$$\begin{aligned} F &= ae^{\log r}, \quad \text{omitting } a \text{ constant,} \\ &= ar, \end{aligned} \tag{3.16}$$

where

$$1 - 2K_0 + K_1a^2 - a^2 = 0,$$

or

$$(1 - A)[(1 - A) - (3 - A)\, a^2] = 0,$$

$$A = 1, \quad a^2 = \frac{1 - A}{3 - A}. \tag{3.17}$$

Thus we see that the value of ϕ is

$$\phi = ar = \sqrt{\frac{1 - A}{3 - A}}\, r, \quad \text{if } A \neq 1. \tag{3.18}$$

4. DETERMINATION OF f

Substituting the value of ϕ from (3.18) in (3.6) we get,

$$\lambda\,[1 - K_0 - \tfrac{1}{2}K_1a^2 - \tfrac{1}{2}a^2 - 2R^2f'^2] - \mu a^2 - 8\mu \int f'^2 dR^2$$
$$- 8\mu \int R^2 f'f'' dR^2 = a \text{ constant.} \tag{4.1}$$

By differentiating (4.1) with respect to $X = R^2$ we get

$$X(\lambda + 2\mu)\frac{df'^2}{dX} + (\lambda + 4\mu)f'^2 = 0, \tag{4.2}$$

which gives

$$f'^2 = \frac{c_1{}^2}{(r^2 + z^2)^{1+c}}, \quad c = \frac{2\mu}{\lambda + 2\mu} \tag{4.3}$$

$$f = \frac{2c_1}{1 - c}(r^2 + z^2)^{\frac{1}{2}(1-c)}, \tag{4.4}$$

neglecting a constant.

The components of displacements now take the form

$$u = r - \alpha r, \; v = \theta - A\theta, \; w = z - \frac{2c_1}{1 - c}(r^2 + z^2)^{\frac{1}{2}(1-c)}, \tag{4.5}$$

where c is the elastic constant $(1 - 2\sigma)/(1 - \sigma)$ and α, A, c_1 are constants to be determined from the boundary conditions and equation (3.17). The non-vanishing stress components are

$$\begin{aligned}
\tau_{rr} &= \lambda\Delta + 2\mu e_{rr} \\
&= \lambda(1 - K_0 - \tfrac{1}{2}K_1a^2 - \tfrac{1}{2}a^2) + \mu(1 - a^2) \\
&\quad - 2\lambda c_1{}^2R^{-2} - 4\mu r^2 c_1{}^2R^{-2(1+c)}, \\
\tau_{\theta\theta} &= \lambda(1 - K_0 - \tfrac{1}{2}K_1a^2 - \tfrac{1}{2}a^2) + \mu(K_0 - \tfrac{1}{2}Ka^2) - 2\lambda c_1{}^2R^{-2}, \\
\tau_{zz} &= \lambda(1 - K_0 - \tfrac{1}{2}K_1a^2 - \tfrac{1}{2}a^2) + \mu - 2\lambda c_1{}^2R^{-2} \\
&\quad - 4\mu z^2 c_1{}^2R^{-2(1+c)}, \\
\tau_{rz} &= -4\mu r z c_1{}^2R^{-2(1+c)}, \\
\tau_{r\theta} &= 0, \quad \tau_{\theta z} = 0.
\end{aligned} \tag{4.6}$$

5. BOUNDARY CONDITIONS FOR A SPHERICAL SHELL

If N denotes the direction of the normal at any point of the shell, the boundary tractions in the direction of r, θ, z corresponding to the general set of displacements given in (2.6) are

$$N_r = \frac{r}{\sqrt{r^2+z^2}}[\lambda\Delta + \mu - 4\mu(r^2+z^2)f'^2] - \frac{\mu\phi_r}{\sqrt{r^2+z^2}}(r\phi_r + z\phi_z), \tag{5.1}$$

$$N_z = \frac{z}{\sqrt{r^2+z^2}}[\lambda\Delta + \mu - 4\mu(r^2+z^2)f'^2] - \frac{\mu\phi_z}{\sqrt{r^2+z^2}}(r\phi_r + z\phi_z), \tag{5.2}$$

$$N_\theta = 0. \tag{5.3}$$

substituting the values of ϕ and f'^2 from (3.18) and (4.3), we get

$$RN_r = r[\lambda(1 - K_0 - \tfrac{1}{2}K_1a^2 - \tfrac{1}{2}a^2) + \mu - \mu a^2 - 2(\lambda+2\mu)c_1{}^2R^{-2c}], \tag{5.4}$$

$$RN_z = z[\lambda(1 - K_0 - \tfrac{1}{2}K_1a^2 - \tfrac{1}{2}a^2) + \mu - 2(\lambda+2\mu)c_1{}^2R^{-2c}]. \tag{5.5}$$

If we assume that the inner surface $R = a$ of the shell is acted upon by a normal traction of the amount $\frac{1}{2}\mu a^2$, we get

$$\lambda(1 - K_0 - \tfrac{1}{2}K_1a^2 - \tfrac{1}{2}a^2) + \mu - 2(\lambda+2\mu)c_1{}^2a^{-2c} = \tfrac{1}{2}\mu a^2. \tag{5.6}$$

Assuming the external surface $R = b$ to be acted on by a traction of amount $\mu a^2 z/b$ in the direction of the axis, we get

$$\lambda(1 - K_0 - \tfrac{1}{2}K_1a^2 - \tfrac{1}{2}a^2) + \mu - 2(\lambda+2\mu)c_1{}^2b^{-2c} = \mu a^2. \tag{5.7}$$

These give

$$c_1{}^2 = \tfrac{1}{8}ca^2\frac{(ab)^{2c}}{b^{2c} - a^{2c}}, \tag{5.8}$$

and

$$\tfrac{1}{4}a^2\left[\frac{ca^{2c}}{b^{2c} - a^{2c}} + (2 - c)\right] = \frac{3}{2} - c - 2K_0(1 - c). \tag{5.9}$$

Also from (3.17) we have

$$(i)\ A = 1,\quad K_0 = \tfrac{1}{2},\quad K_1 = 1. \tag{5.10}$$

$$(ii)\ a^2 = \frac{1 - A}{3 - A}.$$

$$\text{In } (i) \qquad v = 0, \ a^2 = \frac{2(b^{2c} - a^{2c})}{ca^{2c} + (2-c)(b^{2c} - a^{2c})}, \qquad c_1^2 = \tfrac{1}{4}c \frac{(ab)^{2c}}{ca^{2c} + (2-c)(b^{2c} - a^{2c})}. \tag{5.11}$$

In (*ii*) A may be determined from (5.9) and substituted in (5.8) to get c_1^2. Assuming that the plate is bent into a spherical shell with a plane rim, the tractions on the rim are

$$Z_r = \tau_{rz} = -4\mu r z c_1^2 R^{-2(1+c)}, \tag{5.12}$$

$$Z_z = \tau_{zz} = \lambda(1 - K_0 - \tfrac{1}{2}K_1 a^2 - \tfrac{1}{2}a^2) + \mu - 2\lambda c_1^2 R^{-2c} - 4\mu c_1^2 z^2 R^{-2(1+c)}. \tag{5.13}$$

Their statical resultant per unit length of the rim $z = z_0$, is

$$\int_a^b \tau_{zz} \, . \, rdr. = \tfrac{1}{2}\lambda(1 - K_0 - \tfrac{1}{2}K_1 a^2 - \tfrac{1}{2}a^2)(b^2 - a^2) - \frac{\lambda c_1^2}{1-c}(b^{1-c} - a^{1-c}) + \frac{4\mu z_0^2 c_1^2}{c}(b^c - a^c).$$

This is the force which must be applied on the rim to keep the plate in the spherical form.

6. SUMMARY

The use of finite components of strain shows that a plate can be bent into a spherical shell if suitable tractions are applied to the inner and outer surfaces and to the plane rim. The corresponding components of displacement have been obtained.

7. REFERENCES

1. Seth, B. R. .. "Non-linear continuum mechanics," *Proc. Ind. Sci. Congress*, Part II, 1955.
2. ———— .. *Phil. Trans. Roy. Soc. Lond.*, 1935, **234 A**, 231–64.
3. Murnaghan, F. D. .. *Amer. J. Math.*, 1937, **59**, 235.
4. Braun, I. .. *Bull. Res. Counc., Israel*, 1951, **1**, 127.
5. Reiner, M. .. *Appli. Sci. Res.*, 1955, **5 A**, 281.

A NEW SPECTROPHOTOMETRIC METHOD FOR THE DETERMINATION OF COPPER WITH SODIUM VERSENATE

By N. A. Ramaiah and Vishnu

(*Department of Physical Chemistry, Indian Institute of Sugar Technology, Kanpur*)

Received December 26, 1956

(Communicated by Prof. S. N. Gundu Rao, F.A.SC.)

Introduction

Estimation of copper in solutions[1,2] and in a number of alloys[3,4] and metals,[5,6] as also in semi-conductors[7] has been the subject of recent interest. For this purpose a series of reagents like dithizone,[8] thiobenzamide,[1] 2-methyl-8-quinolinol,[9] nitrilotriacetic acid,[10] diethyldithiocarbamate,[5] ethylenediaminetetra-acetic acid (EDTA),[11,12] etc., have been developed for colorimetric estimation of copper. A resumé on the work done, during a period of two years (from August 1953 to August 1955) amounting to a few scores of papers, has been given by Mellon and Boltz.[13]

It is known that EDTA forms a soluble complex with copper[14]; using this property, simple methods for estimation of copper in steel, bronze and other alloys, have been developed. Thus Sedivec and Vasak[15] determined copper in steel by complexing the mixture with EDTA and later precipitating copper with diethyldithiocarbamate. Similarly Byrn and Robertson[16] precipitated copper quantitatively in the presence of EDTA from a solution of nickel copper alloy or bronze by 2-(0-hydroxy phenyl) Benzole. Direct spectrophotometric methods for determining copper with EDTA have also been developed. Malmstadt and Gohrbandt[17] recorded the absorption of copper nitrate versenate and copper versenate solutions in the ultraviolet region and used the absorption at $\lambda = 320$ mμ for estimation of copper with versenate and *vice-versa*. Similarly in the near infra red region Hughes and Mortell[18] showed that copper versenate has its maximum absorption between $\lambda = 700$–750 mμ; employing the absorption of copper at $\lambda = 745$ mμ, Underwood[19] titrated copper solution with EDTA; and Nielsch and Boltz[12] estimated copper with EDTA using the absorption maximum at $\lambda = 720$ mμ.

In the course of a series of investigations on the easy estimation of calcium in sugar solutions and sugarcane juices, which is a problem in sugar technological laboratories, a new method for the estimation of copper spectrophotometrically has been evolved. This method appeared useful

on account of the possibility of using the characteristic absorption of copper in the visible region (at $\lambda = 630$ mμ, *vide infra*). It may be added that there have been similar simple methods worked out (*vide supra*) which involved the use of absorption of copper in the ultraviolet region or in the near infrared. Non-availability of the ultraviolet and other spectrophotometers in our Laboratory set a limitation to the use of these methods. The present communication describes a method for estimation of copper in ammoniacal medium by disodium salt of ethylenediaminetetra-acetic acid using Unicam SP 350 DG Spectrophotometer, which has a continuous variation of wavelength in the region 400–700 mμ.

EXPERIMENTAL

The spectrophotometer employed, *viz.*, Unicam SP 350 DG Spectrophotometer has an one cm. light path.

The substances used were of the following grade: Copper sulphate used was of BDH Analar quality; this was purified by recrystallisation in distilled water.

The sodium versenate employed was of Merck quality.

The method for carrying out the spectrophotometric titrations was as follows: Solutions were made in such a way that the final volume (25 ml.) contained a fixed quantity of copper and ammonia and varying quantities of the titrant, *viz.*, the sodium versenate. The absorption of these solutions was studied in a few cases, in the range 400–700 mμ and in the subsequent experiments at $\lambda = 630$ mμ (*vide infra*).

RESULTS AND DISCUSSION

Figure 1 gives a typical series of results on the absorption of ammoniacal copper solution in the range 400–700 mμ. In this, curves 1, 2 and 3 refer respectively to 20, 16 and 10 mM. concentration of copper solution containing 1·15 M. of ammonia. It was interesting to note that ammoniacal copper solution exhibits well-defined characteristic maximum at $\lambda = 630$ mμ; the absorption at this wavelength obeys Beer's law (*see* Fig. 2) with a value of 50 mole^{-1} litre cm.$^{-1}$ for the corresponding constant. Further, it was instructive to note that the absorption of copper versenate at $\lambda = 630$ mμ also obeyed the Beer's law (Fig. 3); the Beer's constant for copper versenate under the experimental condition, *viz.*, in the ammoniacal medium was 16·7 moles^{-1} litre cm.$^{-1}$ This appreciable difference between the Beer's constants of copper and copper versenate solutions facilitated the execution of the titrations under investigation.

Figure. 4 gives a typical set of curves representing the variation of the absorbency of ammoniacal copper at $\lambda = 630$ mμ during the progress of the

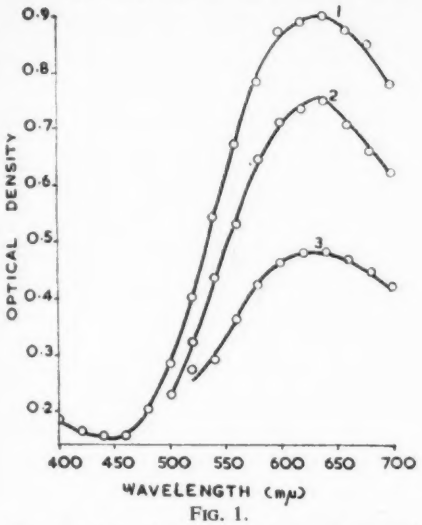

FIG. 1.

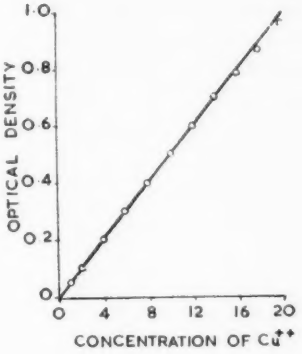

FIG. 2.

FIG. 1. Absorption spectra of copper ammonium complex in the visible region. Concentration of ammonia: 1·15 M. Curve 1 refers to 20 mM.; Curve 2, to 16 mM.; and Curve 3, 10mM. of Cu^{++}.

FIG. 2. Variation of optical density with the concentration of Cu^{++} at $\lambda = 630$ mμ. Concentration of ammonia: 1·15 M. The scale on the X-axis refers to mM.

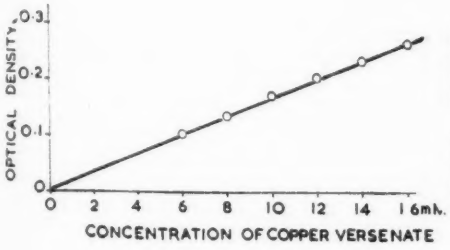

FIG. 3.

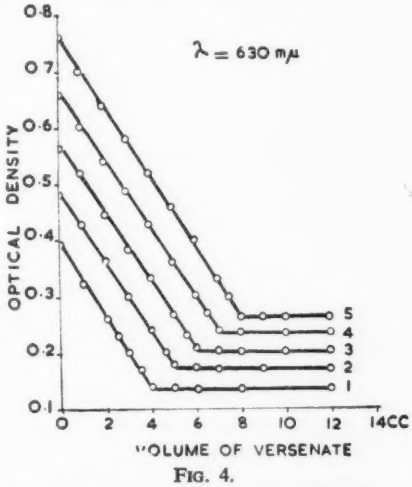

FIG. 4.

FIG. 3. Variation of optical density with the concentration of copper versenate complex at $\lambda = 630$ mμ.
Concentration of ammonia: 1–15 M.

FIG. 4. Spectrometric titration of Cu^{++} with sodium versenate at $\lambda = 630$ mμ.
Concentration of ammonia: 1·15 M. Concentration of sodium versenate: 50 mM. Curve 1 refers to 8 mM.; Curve 2, to 10 mM.; Curve 3, to 12 mM.; and Curve 4, to 16 mM. of Cu^{++}.

titration. It was instructive to note that optical density of copper decreased progressively with the addition of versenate till the end point; further addition of versenate effected little the optical density. It may be noted that the end points were very sharp; the error involved in the determination of copper by versenate is less than 1%.

SUMMARY

Employing the absorption at $\lambda = 630\ m\mu$ of copper ammonium complex, a new method for determination of Cu^{++} by sodium versenate was described. The experimental error involved in the method was less than 1%.

ACKNOWLEDGEMENT

Authors' thanks are due to Professor S. N. Gundu Rao, B.SC., A.H.B.T.I., F.R.I.C., F.A.SC., Director, and to Professor K. S. G. Doss, D.SC., F.R.I.C., F.Inst.P., F.A.SC., Professor of Sugar Chemistry, Indian Institute of Sugar Technology, for their kind interest in the work.

REFERENCES

1. Gagliardi, E. and Haas, W. — *Microchim. Acta*, 1954, **6**, 493.
2. Jewsbury, A. .. — *Analyst*, 1953, **78**, 363.
3. Ellis, K. W. and Gibson, N. A. — *Anal. Chim. Acta*, 1953, **9**, 275.
4. Kalinichenko, I. I. .. — *Zhur. Anal. Khim.*, 1953, **8**, 110.
5. Cluloy, H. J. .. — *Analyst*, 1954, **79**, 561.
6. Guest, R. J. .. — *Anal. Chem.*, 1953, **25**, 1484.
7. Luke, C. L. and Campbell, M. E. — *Ibid.*, 1953, **25**, 1588.
8. Friedeberg, H. .. — *Ibid.*, 1955, **27**, 305.
9. Nievas, J. B. and Berges, L. S. — *Anales real Soc. espań. fis.y. quim (Madrid)*, 1954, **52**, 195.
10. Nielsch, W. and Boltz, G... — *Z. anal. chem.*, 1954, **142**, 406.
11. ———— .. — *Mikrochim. Acta*, 1954, 481.
12. ———— .. — *Z. anal. chem.*, 1954, **143**, 1.
13. Mellon, M. G. and Boltz, D. F. — *Anal. Chem.*, 1954, **28**, 559.
14. Schwarzenbach, G. and Freitag, E. — *Helv. Chim. Acta.*, 1951, **34**, 1503.
15. Sedivec, V. and Vasak, V... — *Coll. Trav. chim Tchecosl.*, 1950, **15**, 260.
16. Byrn, E. E. and Robertson, J. H. — *Anal. Chem.*, 1954, **26**, 1605.
17. Malmstadt, H. V. and Gohrbandt, E. C. — *Ibid.*, 1954, **26**, 442.
18. Hughes, V. L. and Martell, A. E. — *J. Phys. Chem.*, 1953, **57**, 694.
19. Underwood, A. L. .. — *Anal. Chem.*, 1953, **25**, 1910.

THE CRYSTAL STRUCTURE OF MAGNESIUM ACETATE-TETRAHYDRATE $Mg(CH_3COO)_2 . 4 H_2O$

By Jagdish Shankar, P. G. Khubchandani and V. M. Padmanabhan

(Chemistry Division, Atomic Energy Establishment, Bombay)

Received November 16, 1956

(Communicated by Dr. H. J. Bhabha, F.R.S., F.A.SC.)

1. Introduction

Recently Van Niekerk and Schoening[1] have studied the structures of a number of metal acetates. They have stated that direct metal bonds exist in some of these compounds. Magnesium acetate tetrahydrate belongs to the same group as those studied by Niekerk *et al.*, and the present paper gives a report of the investigation of its structure by X-rays.

2. Experimental

The crystals of magnesium acetate were obtained from its aqueous solution by slow evaporation. The crystals were needle-shaped, the long axis being the *c*-axis. The unit cell dimensions, as determined from rotation and Weissenberg photographs, are

$$a = 4{\cdot}75 \text{ Å}, \quad b = 11{\cdot}79 \text{ Å}, \quad c = 8{\cdot}52 \text{ Å} \quad \text{and} \quad \beta = 94° \ 54'.$$

The axial ratios $a : b : c = 0{\cdot}402 : 1 : 0{\cdot}719$ are in good agreement with the previously reported morphological values $a : b : c = 0{\cdot}403 : 1 : 0{\cdot}7128$ and $\beta = 95° \ 37'$ (Groth[2]). Taking the density to be 1·453 (*Hand-book of Chemistry and Physics*) the number of molecules per unit cell is 1·98, *i.e.*, 2. There were no systematic absences in the $h\,k\,l$ reflections showing that the unit cell is primitive. The list of reflecting planes reveals that $0\,k\,0$ is absent when k is odd, and $h\,0\,l$ when l is odd. The space-group is therefore $C_{2h}^5 - P2_1/c$.

Using the multiple film technique, the zero layer Weissenberg photographs were taken on suitable crystal specimens rotating about the *a*- and *b*-axes using Cu-K_α radiation. The intensities of the reflections were estimated visually and corrected in the usual way for the Lorentz and polarisation factors. In view of the small size of the crystals used no corrections were considered necessary for absorption and extinction.

3. DETERMINATION OF THE STRUCTURE

Since the general point position in the $P2_1/c$ is four-fold and as the unit cell contains only two molecules, it follows that the magnesium atoms must be on symmetry centres. The magnesium position was therefore taken at (0, 0, 0). Since the cell dimensions of magnesium acetate and nickel acetate are almost identical, and since they belong to the space-group C_{2h}^5 with the metal atoms at special positions, the signs of the structure factors of magnesium acetate were deduced from those for nickel acctate, taking into consideration the contribution due to the metal atoms. With the signs so obtained a trial Fourier projection on the *bc* plane was made. The projection thus obtained clearly showed the positions of all the atoms and the peaks were well resolved. The maxima were located for all the atoms by Booth's method,[3] and the *y* and *z* co-ordinates of the atoms were estimated. The process was repeated for the *ac* plane, and a Fourier projection was made. Figs. 1 and 2 give the Fourier projections on *bc* and *ac* planes respectively. From these projections the co-ordinates were estimated (Table I).

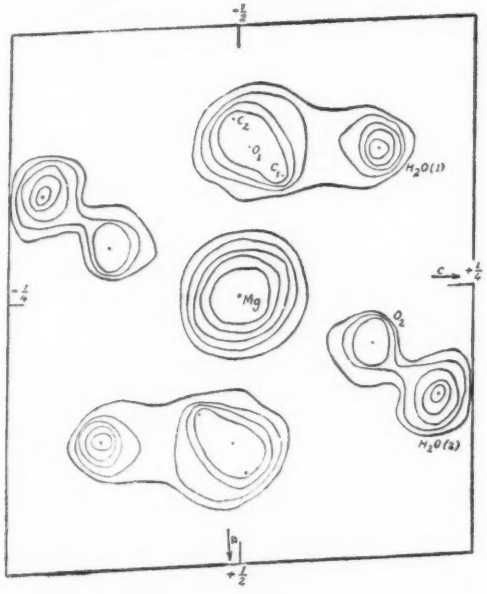

FIG. 1. Fourier projection of the electron density on (*ac*) plane.

With these co-ordinates, structure factors were calculated by allowing for the temperature corrections. The *f*-values for carbon were taken from

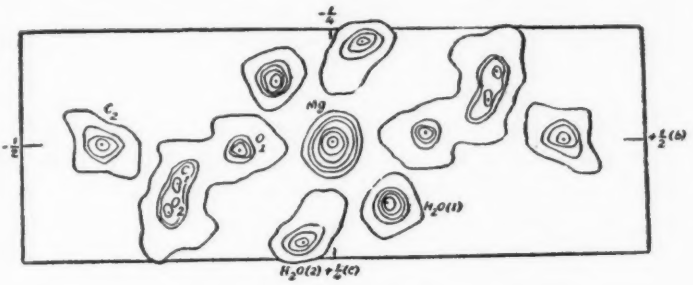

FIG. 2. Fourier projection of the electron density on (*bc*) plane.

TABLE I

Atomic parameters

	x	*y*	*z*
Mg	0·000	0·000	0·000
O_1	−0·250	−0·150	−0·015
O_2	0·067	−0·267	0·150
$H_2O_{(1)}$	−0·283	0·083	0·133
$H_2O_{(2)}$	0·200	−0·050	0·217
C_1	−0·183	−0·250	0·083
C_2	−0·300	−0·367	−0·001

Robertson,[4] for oxygen they were proportionately deduced from Robertsons's values, and for magnesium atom an isotropic temperature factor with $B = 1{\cdot}2$ was used. In Table II, the calculated and observed structure factor values are given. The agreement is good and the Reliability Factor R comes out to be 0·13 for $[(0\,k\,l)]$ zone and 0·21 for $[(h\,0\,l)]$ zone. The bond length and the angles are given in Table III, which were deduced from the atomic co-ordinates given in Table I.

TABLE II

h k l	F_c	F_o	h k l	F_c	F_o	h k l	F_c	F_o
1 0 0	+45	35	0 4 5	+ 4	4	0 12 3	+ 2	4
2 0 0	+35	30	0 4 6	+ 2	6	0 12 4	− 1	3
3 0 0	+17	17	0 5 1	+ 8	11	0 12 5	+ 3	5
4 0 0	+34	26	0 5 2	+21	24	0 13 1	+ 7	5
5 0 0	+ 9	5	0 5 3	+14	19	0 13 5	+ 4	4
0 2 0	− 7	10	0 5 4	− 7	8	1 0 2	+30	24
0 4 0	+17	17	0 5 5	+13	13	1 0 4	+22	19
0 6 0	− 5	5	0 5 6	+ 4	6	1 0 6	+ 5	8
0 8 0	+21	16	0 5 7	+ 2	4	1 0 8	+19	12
0 1 2	+12	12	0 5 8	− 4	6	1 0 10	− 2	4
0 0 2	+34	26	0 5 9	+ 5	6	1 0 $\bar{2}$	−15	11
0 0 4	+22	16	0 6 1	+13	12	1 0 $\bar{4}$	+ 4	5
0 0 6	+32	26	0 6 2	+25	22	1 0 $\bar{6}$	+10	15
0 0 8	+15	12	0 6 3	+ 5	6	1 0 $\bar{8}$	+ 2	4
0 0 10	+17	12	0 6 4	+30	25	2 0 2	− 7	7
0 1 1	+37	33	0 6 6	+12	9	2 0 4	+14	12
0 1 2	+24	22	0 6 8	+ 9	8	2 0 6	+12	15
0 1 3	− 2	4	0 7 1	+14	12	2 0 8	− 2	4
0 1 4	+ 3	2	0 7 2	− 5	3	2 0 $\bar{2}$	+20	16
0 1 5	+18	19	0 7 3	+22	19	2 0 $\bar{4}$	−17	20
0 1 6	+ 5	4	0 7 5	+16	11	2 0 $\bar{8}$	+ 9	7
0 1 7	+ 8	10	0 7 6	+ 4	4	3 0 2	− 8	7
0 1 8	+ 5	6	0 7 7	+10	6	3 0 4	+ 7	9

TABLE II—(*Contd.*)

h k l	F_c	F_0	*h k l*	F_c	F_0	*h k l*	F_c	F_0
0 1 9	+ 9	6	0 7 8	− 2	4	3 0 6	+28	18
0 1 10	− 2	4	0 7 9	+ 7	6	3 0 8	+ 3	4
0 1 11	+ 3	4	0 8 1	+14	14	3 0 $\bar{2}$	+34	24
0 2 2	− 5	5	0 8 2	+24	19	3 0 $\bar{4}$	+11	11
0 2 3	−10	8	0 8 3	+ 3	2	3 0 $\bar{6}$	+ 8	8
0 2 4	+25	20	0 8 4	+11	9	3 0 $\bar{8}$	+16	11
0 2 5	+11	12	0 8 5	− 5	9	4 0 2	+ 4	5
0 2 6	+10	12	0 8 6	+11	8	4 0 4	+ 9	7
0 2 7	+ 4	2	0 8 8	+ 8	5	4 0 6	+15	8
0 2 8	+10	6	0 9 1	+ 4	8	4 0 8	+ 2	3
0 3 1	+17	15	0 9 2	+11	16	4 0 $\bar{2}$	+10	7
0 3 2	−34	34	0 9 3	+13	12	4 0 $\bar{4}$	+12	6
0 3 3	+ 3	5	0 9 5	+ 1	4	4 0 $\bar{6}$	+11	5
0 3 4	− 3	2	0 9 6	+ 6	8	4 0 $\bar{8}$	+ 8	8
0 3 5	+14	15	0 9 7	+ 6	7	5 0 2	− 3	5
0 3 6	+16	14	0 10 1	+ 1	4	5 0 4	+11	8
0 3 8	−12	10	0 10 2	+ 6	7	5 0 6	− 3	4
0 3 9	+ 8	7	0 10 5	+ 1	2	5 0 8	− 6	5
0 3 10	+ 7	8	0 11 1	+13	9	5 0 $\bar{2}$	+ 8	6
0 4 1	+ 9	6	0 11 2	− 8	10	5 0 $\bar{4}$	+ 6	6
0 4 2	+ 8	5	0 11 4	− 5	8	5 0 $\bar{6}$	− 6	5
0 4 3	−15	12	0 11 7	+ 5	6			
0 4 4	− 3	5	0 12 2	+ 9	11			

TABLE III

Bond lengths and angles

O_1–O_2	2·23 Å	Mg–O_1	2·11 Å
O_1–C_1	1·33	Mg–$H_2O_{(1)}$	2·08
O_2–C_1	1·25	Mg–$H_2O_{(2)}$	2·07
C_1–C_2	1·57		
O_1–C_1–O_2	120° 30′		
O_1–Mg–$H_2O_{(1)}$ ..	90° 48′		
$H_2O_{(1)}$–Mg–$H_2O_{(2)}$ ..	88° 48′		

4. CONCLUSIONS

The structure is anologous to that of nickel acetate. The two acetate groups are planar and are distributed with the magnesium atom at a centre of symmetry. Each magnesium atom is surrounded by four water molecules $H_2O_{(1)}$, $H_2O_{(2)}$, $\overline{H_2O_{(1)}}$, $\overline{H_2O_{(2)}}$, and oxygen atoms O_1 and $\overline{O_1}$ (bars denoting the atoms belonging to other acetate group, not shown in the figure). The remaining oxygen atom $O_{(2)}$ is linked to $H_2O_{(2)}$. The acetate group belonging to the magnesium atom situated at $(0, \frac{1}{2}, \frac{1}{2})$ is also linked to the acetate group at (0, 0, 0) by hydrogen bond, as in the case of nickel acetate.

The bond distances between the magnesium atom and water molecules are 2·08 and 2·07 and the distance Mg – O, is 2·11 Å. These are in good agreement with the values obtained in the case of nickel acetate. The $O_1 - C_1$, and $O_2 - C_1$ are found to be 1·33 and 1·25, while in the case of nickel acetate they are reported to be nearly equal.

5. SUMMARY

The crystal structure of magnesium acetate has been completely determined. The crystals are monoclinic with space-group $C_{2h}^5 - P2_1/c$ and two molecules in a unit cell with edges $a = 4·75$ Å, $b = 11·79$ Å, $c = 8·52$ Å and $\beta = 94° 54'$. The positions of the atoms were determined from electron density projections on the *bc* and *ac* planes. From these the various bond lengths and angles were calculated.

6. References

1. Van Niekerk, J. N. and Schoening, F R. L. — *Acta Cryst.*, 1953, **6**, 609.
2. Groth, P. .. *Chemische Krystallographe*, **3**, 64.
3. Booth, A. D. — *Fourier Technique in Organic Structure Analysis*, Cambridge, 1948.
4. Robertson, J. M. .. *Proc. Roy. Soc.*, 1935, **150 A**, 106.

STRUCTURE OF ELASTIN

By G. N. Ramachandran, F.A.Sc. and M. S. Santhanam
(*Department of Physics, University of Madras, Guindy, Madras-25*)

Received December 22, 1956

1. Introduction

Unlike other components of the connective tissue, relatively few structural studies have been reported on elastin. The earliest to investigate the X-ray diffraction pattern of elastin was Kolpak (1935) who found that the unstretched ligament yielded diffuse rings, but on stretching these gave a typical collagen pattern with meridional arcs corresponding to a spacing of 3 A and equatorial spots corresponding to spacings of 11·5 A, 5·9 A and 4·6 A. Astbury (1938, 1940) attributed these results to the presence of small amounts of collagen as impurity in the specimens. According to him, the unpurified fibres of *ligamentum nuchæ* give only an amorphous pattern, but this may be superimposed with the pattern of imperfectly oriented collagen fibres. On stretching, the collagen pattern becomes well oriented. On the other hand, he found that the collagen pattern disappeared if the fibres were treated with hot water over a steam-bath for about a week. On stretching, the amorphous pattern of elastin also showed some signs of orientation parallel to the direction of stretching. Astbury suggested that elastin might be a member of the collagen group whose thermal transformation temperature is below room temperature, but no conclusive evidence was available at that time to decide the question. Bear (1944) recorded small angle patterns of collagen faintly with beef ligament and ascribed these to the presence of very small amounts of collagen as impurity. He suggested that elastin must be excluded from the collagen family (Bear, 1952). Electron microscopic studies (Wolpers, 1944; Gross 1949, 1951; Franchi and de Robertis, 1951) also did not reveal the 640 A spacing typical of collagen or any other fine structure in elastin. The present situation regarding the structure of elastin, as revealed by X-ray and other physical methods, may be summarised as follows (Kendrew, 1953): "Indeed the two main groups of the Astbury classification appear to comprehend virtually all known structure proteins whose X-ray pattern has been examined, with the exception of elastin (a component of some types of elastic tissue) and actin in muscle."

Among the other chemical and other studies on elastin, the following may be mentioned in particular. Lloyd and Garrod (1948) compared the thermoelastic behaviour of elastin and collagen and considered that the

high proportion of non-polar side chains present in elastin would account for the rubber-like properties. Hall *et al.* (1952) suggested that the elastin system at least in parts is made up of linear aggregates of a corpuscular protein unit of low molecular weight called proelastin, analogous to procollagen. Banga and Schuber (1953) have suggested that elastin is a glycoprotein, the fibrous character of which is determined by a carbohydrate group built into the molecule. Later Banga (1953) showed that the reducing substances split off during elastolysis could not be ascribed to carbohydrate. Partridge *et al.* (1955) have suggested that the substance of elementary elastin fibres is a chemically homogeneous protein, although it may exhibit heterogeneity at macromolecular level. The physical properties of the elastic tissue may be a result of the macromolecular structure of elastin comprising the elementary fibres and the way in which the fibres are cemented by collagenous structure and mucoproteins.

During a recent series of studies in this laboratory on the effect of chemical reagents on collagen, it was observed that some of the treated specimens exhibited a very close similarity to elastin in their X-ray pattern as well as in the physical behaviour (unpublished). The change thus produced in collagen was found to be reversible, so that the treated specimen should be considered to be only a modified form of collagen. A careful investigation was therefore made of the relationship between collagen and elastin and the present paper is a report of these studies. It appears that elastin should definitely be classed with collagen and that its molecular structure is also basically built up on the triple chain structure of collagen (Ramachandran and Kartha, 1954, 1955, *a*, *b*; Ramachandran, 1956).

2. X-Ray Patterns of Elastin and Collagen

The X-ray diffraction pattern of elastin supports the suggestion that elastin is closely related to collagen in its structure. The diffraction pattern of elastin, recorded in a 3 cm. cylindrical camera is given in Fig. 1. The pattern in Fig. 1 may be compared with the diffraction patterns of natural collagen fibres (Fig. 2), thermally shrunk collagen (Fig. 3) and gelatin (Fig. 4). The fibres of elastin were obtained from *ligamentum nuchæ* of cattle. The fibres were treated with 20 per cent. sodium chloride solution, washed with distilled water and dehydrated with acetone. Further purification was effected by autoclaving with water. Collagen fibres were obtained from cattle achilles tendon from which soluble proteins were removed by extraction with sodium chloride solution. B.D.H. gelatin was used for obtaining Fig. 4. The thermally shrunk collagen specimen was prepared by heating

a collagen fibre well above the shrinkage temperature and then fixing it in boiling alcohol.

The prominent features of the diffraction pattern of elastin are two diffuse rings of spacings 4·4 A and 2·2 A. While the former was recorded by Astbury using a flat film, the latter has now been observed for the first time. The pattern recorded on a flat film is shown in Fig. 5 and it will be seen from this that there is in addition a central halo, with a faint maximum at about 9–10 A. This feature has also been commented upon by Astbury (1940).

A comparison of Figs. 1 to 4 shows that the 2·2 A ring is common to all, although the other details differ. In fact, there is a close correspondence between the patterns of elastin and thermally shrunk collagen. However, in the patterns of collagen fibre and gelatin, several other reflections occur. Thus, the pattern of collagen fibre exhibits a sharp equatorial reflection at 11 A to 12 A and meridional arcs at 2·86 A and 4 A, and two off-meridional spots corresponding to a spacing of about 7 A. All these reflections occur in the form of rings in the pattern of gelatin. These features are not fully visible in Figs. 2 and 4 since the central region has been overexposed to bring out the 2·2 A ring. Thus, gelatin at room temperature may be considered to be a disoriented (polycrystalline) form of collagen.

The pattern of thermally shrunk collagen differs significantly from those of both normal collagen and gelatin. While the occurrence of complete rings indicates the absence of orientation, as in gelatin, there is a clear indication that it is a more degraded form of collagen than gelatin, since the sharp rings in the pattern of the latter are all absent in the pattern of thermally shrunk collagen.

The sharp reflections corresponding to definite spacings occur in the pattern of collagen fibres because of the high degree of order in its structure. This order is of two types:

(*a*) the order arising from the arrangement of the triple-chain protofibrils in a lattice—the lattice may be a simple hexagonal lattice, or a cylindrical lattice (Ramachandran and Sasisekharan, 1956) but the exact nature is not important for our discussion here.

(*b*) the order arising from the helical arrangement of residues in an individual triple-chain protofibril.

The former leads to the 11A to 12 A equatorial spacing, while the latter is responsible for the 2·86 A meridional arc and also the other spacings.

The 2·86 A corresponds to the tenth order of the repeat distance of 28·6 A spacing along the fibre axis.

It is obvious that the two types of order must be interrelated. An examination of the way in which the triple-chain structure is built up from the amino-acid residues and is stabilised reveals that the exact value of 28·6 A is not demanded by stereochemical or any other considerations connected with a single triple chain. A fairly wide variation, certainly from about 28 A to 31 A, is permissible. Thus, the occurrence of a sharp spacing of 2·86 A must be attributed to the cross-links between *different* protofibrils, which would lead to the repeat spacing being the same in all the protofibrils, and thus producing a high degree of regularity. If for any reason these cross-links are ruptured, then one should observe two effects—(*a*) the equatorial reflection would no longer be sharp, because there is no reason why the protofibrils should be maintained at a constant distance apart, (*b*) the individual protofibrils may also have different values for the repeat spacing along the fibre axis, so that the 2·86 A arc would be rendered diffuse and may even disappear. This is precisely what happens as a result of thermal contraction. The sharp equatorial spots in collagen fibre, which correspond to the 11 A to 12 A ring in cold gelatin, disappear on thermal contraction, and simultaneously the 2·86 A arc and the other sharp reflections or rings also disappear.

The fact that the broad rings at 4·4 A and 2·2 A, which are observed with gelatin, are present in the diffraction pattern of the contracted collagen suggests that the essential triple helical structure is maintained, except that the lattice structure and regularity are lost in the latter. This suggestion is further supported by the fact that thermally contracted collagen may be readily brought to the normal state by stretching it at room temperature.

As already mentioned, the diffraction pattern of elastin is closely similar to that of thermally contracted collagen, and so it is reasonable to suppose that the structure of elastin is also based on the triple-chain collagen structure, in which however the cross-linkages are not present. This happens because elastin contains very few residues with polar side-groups and in particular contains negligible amount of hydroxyproline (Partridge *et al.*, 1955), which is the main cross-linking agent in collagen.

3. Theoretical Considerations

The above observations strongly suggest that the structure of elastin and collagen are closely analogous at the molecular level, and that they are both built up on the triple-helical arrangement proposed from this laboratory (Ramachandran and Kartha, 1955; Ramachandran, 1956). This is

theoretically also very reasonable, for the amino-acid composition of elastin is similar to collagen in two important respects, although there are very few residues with polar side-chains in elastin. It contains slightly more than one-third of glycine and further the proline content is nearly the same as in collagen (Tristram, 1953). The triple-chain structure has the essential property that one-third of the α-carbon atoms cannot have any side-groups attached to them so that the glycine residues must form at least a third of the total number. This is characteristic both of collagen and elastin. So also the five-membered ring of the proline residue can be readily accommodated in the structure. It is interesting that both polyglycine and polyproline are found to take up a configuration similar to the collagen chain (Rich and Crick, 1955; Cowan and McGavin, 1955). Thus a close similarity is to be expected between the structures of collagen and elastin, although so far there is no evidence that every third residue in elastin is glycine or regarding the relative disposition of glycine and proline residues. However, it is possible that the number of residues per turn (which is very nearly $3\frac{1}{3}$ per turn in the minor helix) may not be exactly the same in elastin.

4. Relationship between Elastin and Chemically Treated Collagen

Recently the authors have made a study of the effect of various inorganic salt solutions like those of nickel nitrate and calcium chloride on collagen. Collagen contracts by treatment with these reagents even at room temperature. The progressive transformation of the structure brought about by these reagents has been followed by recording the X-ray patterns after treatment for various intervals of time (unpublished). In the case of both reagents, it is observed that there occurs first a disorientation of the structure and then both the 2·86 A arc and 11 A to 12 A equatorial spots simultaneously disappear. Just after this stage, the pattern of the treated fibres shows a remarkable similarity to that of elastin. Patterns of the calcium chloride treated collagen and of normal elastin recorded on a flat film at 3 cm. are given in Figs. 5 and 6. It will be noticed that the patterns are closely similar and that one could be easily mistaken for the other. The occurrence of a ring at about 9 A to 10 A at the outer edge of the central halo in the pattern of the treated collagen specimen (exactly as with elastin) is particularly noteworthy.

In the nickel nitrate treatment also, the same similarity is observable although there is a general background intensity probably due to the scattering and fluorescent X-rays from nickel in the pattern of this specimen. The ring at 9 A to 10 A has not been observed in the nickel nitrate treated

specimens if the concentration of the solution is large (100 per cent w/v), but the pattern given by them is closely similar to that of thermally shrunk collagen. If a dilute solution of nickel nitrate (30 per cent w/v) is used, and the collagen fibre is treated for a long time (several days), then the X-ray pattern of the fibre is very similar to that of the calcium chloride treated specimen, with a ring at about 9 A at the outer edge of the central halo.

All these specimens also give the 2·2 A diffuse ring if the patterns are recorded in a 3 cm. cylindrical camera. Usually the fibres begin to contract at the stage when the 2·86 A and 11 A to 12 A spots disappear, and they exhibit rubber-like elasticity at this stage.

Further treatment with concentrated nickel nitrate solution causes the disappearance of the halo sorrounding the central spot and the pattern shows only a diffuse ring at 4·4 A with very little intensity inside. This is identical with the pattern of drastically shrunk rat tail tendon recorded by Astbury (1944) and of gelatin sol (high temperature form of gelatin) recorded by Katz *et al.* (1931). Elastin, when treated with nickel nitrate solution for a long time, also gives a pattern identical with the above pattern (*see* Figs. 7 and 8). It may be mentioned that the collagen fibre gives the usual pattern, if it is washed in distilled water, whatever be the stage to which it had been modified by the chemical treatment.

These studies with chemically treated collagen confirm the ideas put forward in the previous sections. The fact that the treated collagen fibres can be readily restored to their normal condition by removing the salt means that the modification induced by the chemical treatment must be very mild. Since the X-ray pattern and physical behaviour of the specimen, treated under appropriate conditions, are very close to those of elastin, it is clear that elastin itself must be very similar to collagen. Further, it is observed that not only can collagen be modified further beyond this stage, when its X-ray pattern is similar to that of elastin, to that corresponding to hot gelatin, but elastin also exhibits such a change when treated with nickel nitrate. In fact, drastic thermal treatment also produces such a change in elastin, exactly as with drastically thermally shrunk collagen. If elastin is autoclaved and immediately the X-ray pattern is recorded, the pattern is identical with that of the drastically shrunk collagen, both showing only a fairly sharp ring at 4·5 A, with practically clear region within. This photograph is not reproduced, but is very similar to Fig. 7 (*a*) of Astbury's paper (1940) of rat tail tendon contracted to about 17 per cent. of its initial length.

Similarly, it has been observed that if elastin is kept wet and the X-ray pattern taken, the pattern is very similar to that of wet gelatin. Thus, not only is it possible to produce a material from collagen which is very similar to elastin, but the further changes produced in both are also very similar. All these clearly show that elastin in fact belongs to the collagen family of proteins.

5. OTHER OBSERVATIONS ON COLLAGEN AND ELASTIN

When the above studies were nearing completion, an interesting article by Burton *et al.* (1955) appeared, in which an apparent transformation of collagen fibres into a structureless elastin-like material was observed, when collagen was treated with some chemical reagents like borate buffer solutions. However, these authors have not observed the re-formation of the collagen, when the chemical is washed off.

The similarity of shrunk collagen and elastin has also been observed by Banga (1953) who found that collagen is attacked and solubilised by elastase if it has been shrunk thermally or by treatment with phosphotungstic acid, but is unattacked in the normal state.

In view of the evidences from different sources, it appears to be very likely that proteins with properties and composition intermediate between those of collagen and elastin could also occur in biological systems (*cf.* Burton *et al.*, 1955). It would be interesting to examine if this is so. The X-ray patterns of immature and developing collagenous tissue recorded by North *et al.* (1953) appear to support this idea. With increase of age of rats, the pattern of the tail tendon is found to change from the elastin-shrunk collagen type to the normal collagen type. So also the infra-red data of developing tendon given by Jackson *et al.* (1953) show that the NH stretching frequency (3310 $cm.^{-1}$) of the developing tendon is significantly lower than that of adult tendon (3330 $cm.^{-1}$) and agrees with the value observed for hot gelatin (Robinson, 1953). It would be interesting to examine if elastin itself shows the lower frequency since the present studies indicate the similarity of the structure of elastin to degraded and less developed forms of collagen. So far no infra-red data on elastin appear to have been reported.

Thus, elastin is probably a precursor of collagen in biological systems and collagen may be formed by the incorporation of polar residues and the resulting formation of cross-linkages. Burton *et al.* (1955) have on the other hand suggested that elastin is produced *in vivo* by degradation of collagen, although some of the co-authors (Hall *et al.*, 1955) themselves are of the view that this is probably less reasonable biologically than the reverse process.

6. Summary

The paper deals with the structure of elastin and its relationship to collagen. It is shown that, on the molecular level, elastin is analogous to collagen and is built up on a triple-chain helical arrangement of amino-acid residues. It is possible to obtain a material yielding an X-ray diffraction pattern very similar to elastin, by treating collagen with calcium chloride solution. The relationship between elastin and collagen in biological systems is also discussed.

7. Acknowledgement

The authors express their grateful thanks to Prof. W. T. Astbury for valuable discussions by correspondence.

8. References

Astbury, W. T. ..	*Trans. Far. Soc.*, 1938, **34**, 378.
———— ..	*J. Int. Soc. Leather Trades' Chemists*, 1940, **24**, 69.
Banga, I. ..	*Nature*, 1953, **172**, 1009.
—— and Schuber, D. ..	*Acta Physiol. Hung.*, 1953, **4**, 14.
Bear, R. S. ..	*J. Amer. Chem. Soc.*, 1944, **66**, 1297.
———— ..	*Advances in Protein Chem.*, 1952, **7**, 89.
Burton, D., Hall, D. A., Keech, M. K., Reed, R., Saxl, H. and Tunbridge, R. E.	*Nature*, 1955, **176**, 966.
Cowan, P. M. and McGavin, S.	*Ibid.*, 1955, **176**, 264.
Franchi, C. M. and de Robertis, E.	*Proc. Soc. Exptl. Biol. Med.*, 1951, **76**, 515.
Gross, J. ..	*J. Exptl. Med.*, 1949, **89**, 699.
———— ..	*Proc. Soc. Exptl. Biol. Med.*, 1951, **78**, 241.
Hall, D. A., Reed, R. and Tunbridge, R. E.	*Nature*, 1952, **170**, 264.
——, Keech, M. K., Reed, R. Saxl, H., Tunbridge, R. E. and Wood, M. J.	*J. Geront.*, 1955, **4**, 388.
Jackson, F. S., Kelly, F. C., North, A. C. T., Randall, J. T., Seeds, W. E., Watson, M. and Wilkinson, G. R.	*Nature and Structure of Collagen*, Butterworths, London, 1953, p. 106.
Lloyd, D. J. and Garrod, M. ..	*Trans. Far. Soc.*, 1948, **64**, 441.
Katz, J. R., Derksen, J. C. and Bon, W. F.	*Rec. Trav. Chim.*, 1931, **50**, 725, 1138.
Kendrew, J. C. ..	*The Proteins*, Academic Press, New York, 1953, **2B**, 848.
Kolpak, H. ..	*Koll. Z.*, 1935, **73**, 129.

Partridge, S. M., Davis, H. F. and Adair, G. S. — *Biochem. J.*, 1955, **61**, 11.

Ramachandran, G. N. and Kartha, G. — *Nature*, 1954, **174**, 269.

———— .. *Ibid.*, 1955, **176**, 593.

———— .. *Proc. Ind. Acad. Sci.*, 1955, **42 A**, 216.

Ramachandran, G. N. .. *Nature*, 1956, **177**, 710.

——— and Sasisekharan, V. .. *Arch. Biochem. Biophys.*, 1956, **63**, 255.

Rich, A. and Crick, F. H. C. .. *Nature*, 1955, **176**, 780.

Robinson, C. .. *Nature and Structure of Collagen*, Butterworths, London, 1953, p. 96.

Tristram, G. R. .. *The Proteins*, Academic Press, New York, 1953, **1A**, 221.

Wolpers, C. .. *Klin. Wochschr.*, 1944, **23**, 169.

DESCRIPTION OF PLATES

PLATE II

All the photographs have been taken with CuKα radiation in a crylindrical camera (R = 3 cm.)

FIG. 1. Elastin.

FIG. 2. Collagen fibre.

FIG. 3. Thermally shrunk collagen.

FIG. 4. Gelatin.

PLATE III

FIG. 5. X-ray diffraction pattern of calcium chloride treated collagen (Flat film, $d = 3$ cm.).

FIG. 6. X-ray pattern of elastin (Flat film, $d = 3$ cm.).

FIG. 7. X-ray pattern of nickel nitrate treated collagen (Flat film, $d = 5$ cm.).

FIG. 8. X-ray pattern of nickel nitrate treated elastin (Flat film, $d = 5$ cm.).

FIG. 1

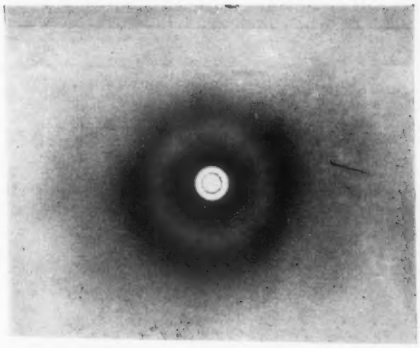

FIG. 2

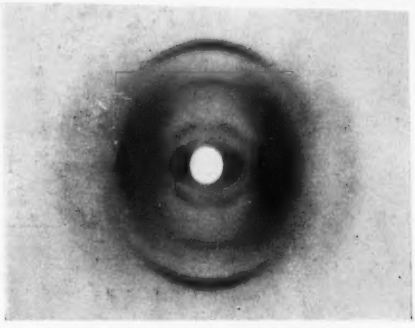

FIG. 3

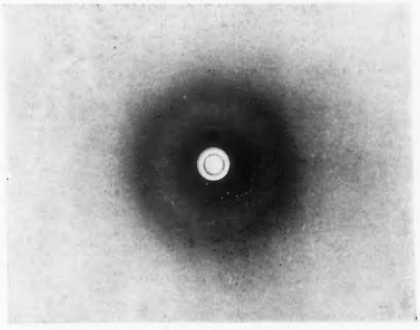

FIG. 4

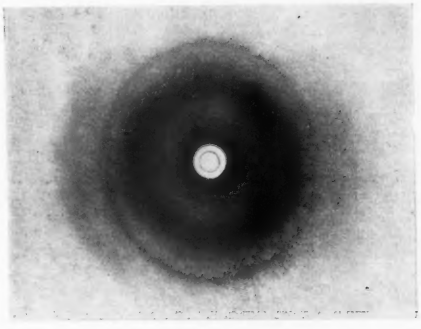

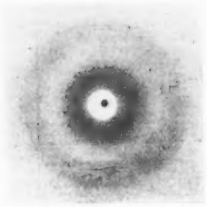

FIG. 5

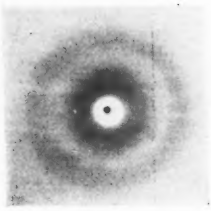

FIG. 6

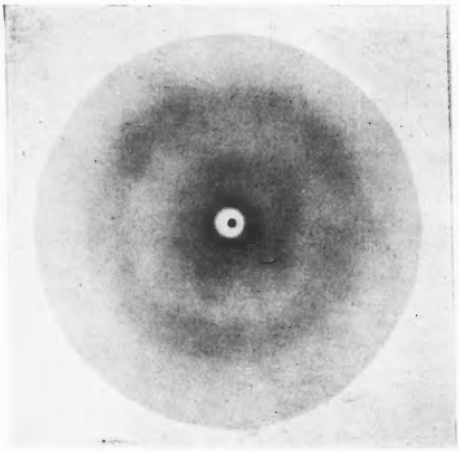

FIG. 7

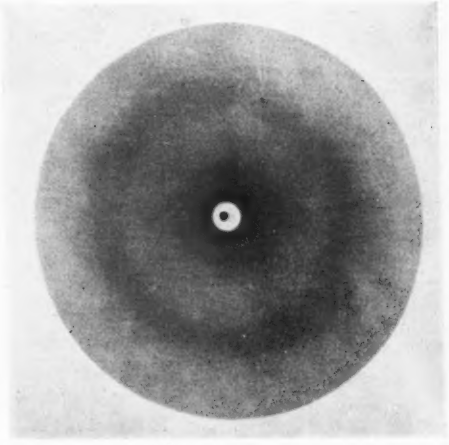

FIG. 8

A NOTE ON CASCADE THEORY WITH IONISATION LOSS

By Alladi Ramakrishnan, F.A.Sc. and S. K. Srinivasan
(*Department of Physics, University of Madras*)

Received January 3, 1957

Abstract

The cascade theory of cosmic ray showers including ionisation loss is dealt with on the basis of the new approach suggested by us in an earlier contribution and an explicit Mellin transform solution is obtained for the mean number of particles produced in an infinite thickness of matter.

Some years ago, Bhabha and Chakrabarthy (1943) obtained and discussed the equations of the cascade theory expressing the mean behaviour of the particles when collision loss is also taken into account. If $f(E; t)\,dE$ and $g(E; t)\,dE$ are the mean numbers in the energy interval dE of electrons and photons respectively and $R(E'|E)$ and $\rho(E'|E)$ are the cross-sections for radiation and pair-production respectively, the equations are

$$\frac{\partial f(E;t)}{\partial E} = -f(E;t)\int_0^E R(E'|E)\,dE' + \int_E^\infty f(E';t)\,R(E|E')\,dE' + 2\int_E^\infty g(E';t)\,\rho(E|E')\,dE' + \beta\frac{\partial f(E;t)}{\partial E} \tag{1}$$

$$\frac{\partial g(E;t)}{\partial t} = -g(E;t)\int_0^E \rho(E'|E)\,dE' + \int_E^\infty f(E';t)\,R(E'-E|E')\,dE' \tag{2}$$

with the initial conditions

$$f(E;0) = \delta(E - E_0) \tag{3}$$

where δ is the Dirac delta function and

$$g(E;0) = 0 \tag{4}$$

corresponding to a shower excited by a single electron of energy E_0. In conformity with the theory of 'product densities'* (which is usually useful for obtaining higher moments of the distribution) we recognise f and g as

* For a formulation of the theory of product densities, *see* Ramakrishnan (1950).

the product densities of degree one of electrons and photons at t. The collision loss in traversing unit thickness of matter is assumed to be a constant, β. Defining the Mellin transforms of $f(\mathrm{E};t)$ and $g(\mathrm{E};t)$ as

$$p(s;t) = \int_0^\infty f(\mathrm{E};t)\,\mathrm{E}^{s-1}d\mathrm{E} \tag{5}$$

$$q(s;t) = \int_0^\infty g(\mathrm{E};t)\,\mathrm{E}^{s-1}d\mathrm{E} \tag{6}$$

according to Bhabha and Chakrabarthy, equations (1) and (2) can be reduced to

$$\frac{\partial p(s;t)}{\partial t} = -\mathrm{A}_s\,p(s;t) + \mathrm{B}_s\,q(s;t) - (s-1)\,\beta p(s-1;t) \tag{7}$$

$$\frac{\partial q(s;t)}{\partial t} = \mathrm{C}_s\,p(s;t) - \mathrm{D}q(s;t) \tag{8}$$

A_s, B_s, C_ε and D are given by (*see* Bhabha and Chakrabarthy, 1943)

$$\mathrm{A}_s = \left(\frac{4}{3}+\alpha\right)\left\{\frac{d}{ds}\log\overline{s} + \gamma - 1 + \frac{1}{s}\right\} + \tfrac{1}{2} - \frac{1}{s(s+1)}$$

$$\mathrm{B}_s = 2\left\{\frac{1}{s} - \left(\frac{4}{3}+\alpha\right)\frac{1}{(s+1)(s+2)}\right\}$$

$$\mathrm{C}_s = \frac{1}{s+1} + \left(\frac{4}{3}+\alpha\right)\frac{1}{s(s-1)}$$

$$\mathrm{D} = \frac{7}{9} - \frac{1}{6}\alpha \tag{9}$$

We note that (7) is a difference-differential equation where the difference relates to the complex variable s and hence cannot be solved by direct iteration. Moreover the dependence on t makes the solution much more difficult. A simple question that can be asked is: What is the spectrum at $t = \infty$? Unfortunately the product density functions $f(\mathrm{E};t)$ and $g(\mathrm{E};t)$ tend to zero as $t \to \infty$ (for $\mathrm{E} > 0$) and thus nothing interesting can be obtained. However on the basis of the new approach suggested by us in a previous paper (1956) we can ask for the mean number of particles produced in the entire shower, each of the particles having an energy greater than E_c at the point of its production. We shall show that explicit Mellin transform solution for the mean number of particles in this case can indeed be obtained using standard mathematical techniques.

Let $F(E; t)\,dEdt$ and $G(E; t)\,dEdt$ be the mean numbers of elcetrons and photons produced between t and $t + dt$ respectively with their energies at the points of their production lying between E and $E + dE$. $F(E; t)$ and $G(E; t)$ are product densities of degree one with respect to the two variables E and t. Using elementary probability arguments as we have done in our previous paper, we obtain

$$F(E; t) = 2\int_{E}^{\infty} g(E'; t)\,\rho(E|E')\,dE' \tag{10}$$

$$G(E; t) = \int_{E}^{\infty} f(E'; t)\,R(E' - E|E')\,dE' \tag{11}$$

Note that (10) and (11) are valid whether or not we take ionisation loss into account. In fact, the dependence of F and G on ionisation loss enters through f and g.

(10) and (11) are amenable to the standard Mellin transform technique. Defining $P(s; t)$ and $Q(s; t)$ as the Mellin transforms with respect to E, we find

$$P(s; t) = \int_{0}^{\infty} F(E; t)\,E^{s-1}dE = B_s\,q(s; t) \tag{12}$$

$$Q(s; t) = \int_{0}^{\infty} G(E; t)\,E^{s-1}dE = C_s\,P(s; t). \tag{13}$$

The mean numbers of electrons and photons produced in the shower between 0 and t with the 'primitive' energies (energy at the point of production) lying above E_c is given by

$$\epsilon\{N(E_c; t)\} = \frac{1}{2\pi i}\int_{0}^{t} d\tau \int_{E_c}^{\infty} dE \int_{\sigma - i\infty}^{\sigma + i\infty} P(s; \tau)\,E^{-s}ds \tag{14}$$

$$\epsilon\{M(E_c; t)\} = \frac{1}{2\pi i}\int_{0}^{t} d\tau \int_{E_c}^{\infty} dE \int_{\sigma - i\infty}^{\sigma + i\infty} Q(s; \tau)\,E^{-s}ds \tag{15}$$

That these expressions tend to finite limits as $t \to \infty$ is obvious from a physical point of view since the number of particles with non-zero primitive energy by an initial particle of finite energy must be finite. Inverting the order of integrations we write the limits as

$$\epsilon\{N(E_c; \infty)\} = \frac{1}{2\pi i}\int_{\sigma - i\infty}^{\sigma + i\infty} \frac{E_c^{-s+1}}{s - 1}\,B_s ds \int_{0}^{\infty} q(s; \tau)\,d\tau \tag{16}$$

$$\epsilon\{M(E_c; \infty)\} = \frac{1}{2\pi i}\int_{\sigma-i\infty}^{\sigma+i\infty} \frac{E_c^{-s+1}}{s-1}\, C_s ds \int_0^\infty p(s;\tau)\, d\tau \tag{17}$$

Thus the problem of obtaining the mean numbers reduces to that of solving for $\kappa_1(s)$ and $\kappa_2(s)$ where

$$\kappa_1(s) = \int_0^\infty p(s;\tau)\, d\tau$$

$$\kappa_2(s) = \int_0^\infty q(s;\tau)\, d\tau \tag{18}$$

We next proceed to show that though we cannot obtain explicit solutions of $p(s; t)$ and $q(s; t)$ from (7) and (8), we can solve for $\kappa_1(s)$ and $\kappa_2(s)$ quite easily. Integrating both sides of equations (7) and (8) with respect to t from 0 to ∞ and observing that $p(s; 0) = E_0^{s-1}$ and $q(s; 0) = 0$ we obtain

$$-E_0^{s-1} = A_s\kappa_1(s) + B_s\kappa_2(s) - (s-1)\beta\kappa_1(s-1) \tag{19}$$

$$0 = C_s\kappa_1(s) - D\kappa_2(s) \tag{20}$$

Eliminating $\kappa_2(s)$, we have

$$-E_0^{s-1} = -A_s\kappa_1(s) + \frac{B_sC_s}{D}\kappa_1(s) - (s-1)\beta\kappa_1(s-1) \tag{21}$$

i.e.,

$$\kappa_1(s) = \frac{E_0^s + \left(\frac{C_{s+1}B_{s+1}}{D} - A_{s+1}\right)\kappa_1(s+1)}{\beta s} \tag{22}$$

This recurrence relation can be continued and we have

$$\kappa_1(s) = \sum_{r=0}^{m-1} \frac{E_0^{s+r}\left(\frac{C_{s+1}B_{s+1}}{D} - A_{s+1}\right)\left(\frac{C_{s+2}B_{s+2}}{D} - A_{s+2}\right)\cdots\left(\frac{C_{s+r}B_{s+r}}{D} - A_{s+r}\right)}{\beta^r s(s+1)\cdots(s+r)}$$

$$+ \frac{\left(\frac{C_{s+1}B_{s+1}}{D} - A_{s+1}\right)\left(\frac{C_{s+2}B_{s+2}}{D} - A_{s+2}\right)\cdots\left(\frac{C_{s+m}B_{s+m}}{D} - A_{s+m}\right)}{\beta^m s(s+1)\cdots(s+m)} \tag{23}$$

From (22), we note $\kappa_1(s+m)$ for very large m is given by

$$\kappa_1(s+m) \simeq \frac{E_0^{s+m}}{\beta s + A_{s+m}} \tag{24}$$

so that the last term in (23) is negligible if m is sufficiently large. Hence we can write formally

$$\kappa_1(s) = \sum_{r=0}^{\infty} \frac{E_0^{s+r} \prod_{i=1}^{r} (C_{s+i}B_{s+i} - DA_{s+i})}{(\beta D)^r s(s+1)\cdots(s+r)} \tag{25}$$

We shall show that the infinite series on the R.H.S. of (25) does converge absolutely so that (25) is the solution for $\kappa_1(s)$.
Writing

$$\kappa_1(s) = \sum_{m=0}^{\infty} \phi(m) \tag{26}$$

we find

$$\frac{\phi(m)}{\phi(m+1)} = \frac{D\beta}{E_0} \cdot \frac{s+m}{C_{s+m}B_{s+m} - DA_{s+m}} \tag{27}$$

For very large values of m, C_{s+m} and B_{s+m} are negligible and hence we write

$$\frac{\phi(m)}{\phi(m+1)} = -\frac{\beta}{E_0} \cdot \frac{s+m}{A_{s+m}} \tag{28}$$

For large m

$$A_{s+m} \simeq \left(\frac{4}{3} + a\right)\left(\frac{d}{dz}\log \overline{|z}\right)_{z=s+m} \tag{29}$$

The asymptotic expression for $d/dz \log \overline{|z}$ can be derived by standard techniques [*see* for example Jeffreys and Jeffreys (1950), p. 466] as

$$\frac{d}{dz}\log \overline{|z} \simeq \log z + \frac{1}{2z} \tag{30}$$

Thus

$$\left|\frac{\phi(m)}{\phi(m+1)}\right| \simeq \frac{\beta}{E_0}\left(\frac{4}{3} + a\right)^{-1}\left|\frac{s+m}{\log(s+m)}\right| \tag{31}$$

so that

$$\left|\frac{\phi(m)}{\phi(m+1)}\right|$$

tends to infinity as $m \to \infty$. Hence the series $\Sigma\phi(m)$ converges absolutely.

Substituting (25) into (15) and (16), we find

$$\epsilon\{N(E_c; \infty)\} = \frac{1}{2\pi i}\sum_{m=0}^{\infty} \frac{E_0^{m+1}}{(\beta D)^m} \int_{\sigma-i\infty}^{\sigma+i\infty} \left(\frac{E_0}{E_c}\right)^{s-1} \frac{B_s C_s}{D(s-1)}$$

$$\cdot \frac{\prod_{i=1}^{m} \pi (C_{s+i} B_{s+i} - D A_{s+i})}{s(s+1) \cdots (s+m)} \, ds \tag{32}$$

$$\epsilon \{M(E_c; \infty)\} = \frac{1}{2\pi i} \sum_{m=0}^{\infty} \frac{E_0^{m+1}}{(\beta D)^m} \int_{\sigma - i\infty}^{\sigma + i\infty} \left(\frac{E_0}{E_c}\right)^{s-1} \frac{B_s}{s-1}$$

$$\cdot \frac{\prod_{i=1}^{m} \pi (C_{s+i} B_{s+i} - D A_{s+i})}{s(s+1) \cdots (s+m)} \, ds \tag{33}$$

We note that the series in (32) and (33) contains inverse powers of β as contrasted with the assumed expansion in terms of positive powers of β obtained by Bhabha and Chakrabarthy (1943, 1948). It is interesting to note that in the case of a simple multiplicative model discussed in connection with the theory of multiple points by us elsewhere, the solution for the mean number is also a series of inverse powers of β.

We are thankful to Dr. V. K. Balachandran for discussions regarding the validity of our iterative procedure.

One of us (S. K. S.) is grateful to the University of Madras for a Government of India Scholarship.

REFERENCES

1. Bhabha, H. J. and Chakrabarthy, S. K. — *Proc. Roy. Soc.*, 1943, **181 A**, 264.
2. ———— .. *Phys. Rev.*, 1948, **74**, 1352.
3. Jeffreys, H. and Jeffreys, B. S. — *Methods of Mathematical Physics*, Cambridge, 1950.
4. Ramakrishnan, Alladi and Srinivasan, S. K. — *Proc. Ind. Acad. Sci.*, 1956, **44**, 263.
5. Ramakrishnan, Alladi .. *Proc. Camb. Phil. Soc.*, 1950, **46**, 595.

142–57. Printed at The Bangalore Press, Bangalore City, by C. Vasudeva Rao, Superintendent, and Published by The Indian Academy of Sciences Bangalore.

NOTICE TO AUTHORS

Scientific papers intended for publication in the *Proceedings of the Indian Academy of Sciences* can be accepted only when they are communicated by a Fellow of the Academy whose duty shall be to satisfy himself that such communications are fit to be read at the Meeting of the Academy and published in its *Proceedings*.

Papers should not ordinarily exceed fifty pages of foolscap. MSS. should be either typewritten or written in legible hand on one side of the paper. All papers should be carefully revised by the authors and should be absolutely in final form for printing. Position for text-figures should be indicated. Each paper shall conclude with a critical summary not exceeding 350 words.

Drawings, diagrams or other illustrations should be made on larger scale (preferably) twice the size than the ones in which they are intended to appear. They should be done in Indian ink on bristol board with lettering in pencil. Scale of magnification of camera lucida tracings should be indicated by the side of drawings. In certain special cases arrangements will also be made for monochrome lithographic and other colour plates. Reduction of illustrations desired should be indicated in pencil. Appropriate legends should accompany all drawings. Names of authors are to be marked in pencil on the left-hand corner of drawing sheets. Photomicrographs should be securely mounted with colourless paste.

All tables, quotations and footnotes which will be set hereafter (beginning from Vol. I, No. 2) in types smaller than the text, should be typewritten on separate sheets and placed with the text in proper sequence. Footnotes should be numbered in Arabic numerals.

References to literature in the text should be given, whenever possible, in chronological order, only the names of authors and years of publication, in brackets, being given. They should be cited in full after the summary, the authors' names following in alphabetical order. Thus,

Name or Names of author; Name of Journal (abbreviation) with a single underline; Year of publication; Number of Volume with a double underline, and lastly page. The following would be a useful illustration:—

Bergmann and Stather . . . . . Z. Physiol. Chem., 1926, 152, 189.

Two copies of slip-proof and wherever possible, a page proof for final revision will be sent to authors. All corrections are best made on the slip-proof which should be transmitted to the Office of the Academy. All proof corrections involve heavy expenses which would be negligible if the papers are carefully revised by the authors before submission.

Fifty free reprints including plates and with cover will be supplied for each paper. Additional copies can be supplied at cost on previous intimation.

Blocks appearing in the *Proceedings* will be available for purchase by their respective authors. Orders for the same should be sent along with the corrected proofs and in any case not later than one month after the date of publication of the paper. The price charged would be 25% of the actual cost of the blocks *plus* freight and despatching charges. If the blocks are reproduced in other journals or publications, due acknowledgment should be made in them to the *Proceedings*.

The original drawings and plates of blocks appearing in the *Proceedings* will be returned to such of the authors as may require them provided the cost of despatching such originals is borne by them.

CONTENTS

PAGE

The Specific Heats of Some Metallic Elements. Part III. The Characteristic Frequencies . . . . . Sir C. V. Raman 59

Oxidations with Silver Iodide Dibenzoate. Part II. Preparation of *s*-Azo Compounds from Some Aromatic Primary Amines . . . P. S. Raman 65

Numerical Calculations on the New Approach to the Cascade Theory—I . . . . . S. K. Srinivasan and N. R. Ranganathan 69

On the Determination of the Slowing Down Length in Ordinary Water Using A Pulsed Neutron Source . . . R. Ramanna and M. P. Navalkar 74

The Characteristic Roots of the Product of Matrices . . . . N. A. Khan 84

Improvements in Colorimetric Determinations. III. Comparison of Colorimetric and Electrometric Methods for the Determination of Soil Reaction . . . . . K. L. Khanna, P. B. Bhattacharya and K. Prasad 89

Polarographic Studies on the Composition of Nickel Ferrocyanide Complex . . . . . H. C. Saraswat and S. K. D. Agarwal 91

Chromatographic Studies on the Kinetics of the Production of Caramel . . . . . N. A. Ramaiah, S. K. D. Agarwal and J. K. P. Agarwal 97

New Solutions for Finite Deformation . . . . . B. R. Seth 105

A New Spectrophotometric Method for the Determination of Copper with Sodium Versenate . . . . . N. A. Ramaiah and Vishnu 113

The Crystal Structure of Magnesium Acetate-Tetrahydrate $Mg(CH_3COO)_2 . 4H_2O$ . . . . . Jagdish Shankar, P. G. Khubchandani and V. M. Padmanabhan 117

Structure of Elastin. . . . . G. N. Ramachandran and M. S. Santhanam 124

A Note on Cascade Theory with Ionisation Loss . . . . . Alladi Ramakrishnan and S. K. Srinivasan 133

CE
59
65
69
74
84
89
91
97
105
113
117
124
133